THE EFFECT OF MGAT EXPRESSION ON CELLULAR LIPID METABOLISM

By

Kyong Jin Ahn

A thesis submitted to the

Graduate School-New Brunswick

Rutgers, The State University of New Jersey

in partial fulfillment of the requirements

for the degree of

Master of Science

Graduate Program in Nutritional Sciences

written under the direction of

Dr. Judith Storch

and approved by

_____

_____

_____

_____

New Brunswick, New Jersey

October, 2010

ABSTRACT OF THE THESIS

THE EFFECT OF MGAT EXPRESSION ON CELLULAR LIPID METABOLISM

by KYONG JIN AHN

Thesis Director:

Judith Storch, PhD

Following absorption into the enterocyte, free fatty acid (FFA) and *sn*-2-monoacylglycerol (*sn*-2-MG), the major hydrolysis products of dietary lipids, are reconstituted to triacylglycerol (TG) by the monoacylglycerol acyltransferase (MGAT) pathway, which is the primary TG synthesis pathway in the postprandial condition. Nevertheless, the precise function and contribution of the MGAT pathway to lipid synthesis are not fully understood. Therefore in this study, we examined the effect of MGAT expression on cellular lipid metabolism.

Although the Caco-2 cell line, which is derived from human colorectal cancer cells, is the most relevant in vitro model to examine the influence of hMGAT2 expression on lipid metabolism in the enterocyte, we could not obtain any definitive metabolism data caused by MGAT expression due to their inconsistent transfection efficiency. Thus we transiently expressed hMGAT2 in CHO-K1 cells, which are relatively easier to transfect, and these cells were then used to study the metabolism of radiolabeled FFA or sn-2-MG.

Empty vector-transfected (mock) and MGAT-transfected cells, which were incubated with FA, showed the increased net uptake as a function of time, and both groups metabolized most of absorbed FA to phospholipid (PL). Between the two groups, there were no significant differences. In contrast, MGAT expressing cells which were incubated with MG, absorbed remarkably higher amounts of lipid relative to mock-transfected cells. This suggests that MGAT

expression promotes the rapid uptake of MG across the membrane by efficiently maintaining concentration gradients, or that the transmembrane lipid transport proteins are influenced by MGAT expression. The incorporation of absorbed MG into each lipid class was also significantly different between mock and MGAT expressing cells. More MG was incorporated into TG and DG in the MGAT transfected cells. In addition, the MGAT expressing cells showed higher percent incorporation into PL and lower percent incorporation into TG comparing to mock expressing cells. This difference in metabolic channeling suggests that diacylglycerol (DG) synthesized from MGAT pathway may not be equivalent with DG synthesized from G-3-P pathway, which is the ubiquitous metabolic pathway used to synthesize TG in most cells.

We therefore suggest that MGAT expression may increase the net uptake of lipid into cells, and that the G-3-P and MGAT pathways may have different pools of DG which are metabolized to PL or TG.

Acknowledgements

I would like to show gratitude to my thesis advisor Dr. Judith Storch for her dedication, encouragement, and patient guidance throughout the study. I also would like to appreciate my thesis committee, Drs. Dawn Brasaemle and Ariel Igal, for their critical readings. In addition, I really thank all the members in Dr. Storch's lab for their support. Lastly, I am deeply thankful to my friends and family for their patient support and kindness.

Table of contents

List of tables

List of figures

List of abbreviations

ACAT	Acyl CoA: cholesterol acyltransferase
AP	Apical
BBM	Brush border membrane
BL	Basolateral
CE	Cholesterol ester
CEL	Carboxyl ester lipase
CM	Chylomicron
CMC	Critical micellar concentration
DG	Diacylglycerol
DGAT	Diacylglycerol acyltransferase
ER	Endoplasmic reticulum
FA	Fatty acid
FABPpm	Plasma membrane fatty acid binding protein
FATP	Fatty acid transport protein
G-3-P	Glycerol-3-phosphate
GPAT	Glycerol-3-phosphase acyltransferase
HSL	Hormone sensitive lipase
IFABP	Intestinal fatty acid binding protein
LCFA	Long chain fatty acid
LFABP	Liver fatty acid binding protein
MG	Monoacylglycerol
MGAT	Monoacylglycerol acyltransferase
PC	Phospatidylcholine
PL	Phospholipid

PTL	Pancreatic triacylglycerol lipase
TG	Triacylglycerol
UWL	Unstirred water layer
VLDL	Very low density lipoprotein

Chapter I. Introduction

The human gut is a 10 meter long inner-lining tube. It is one of the body's most specialized systems. Gut is sporadically exposed to huge amounts of foodstuffs, and systematically extracts essential nutrients from this overflow of nutrients (1).

A typical Western diet contains 100-150 g of dietary lipids per day, which is mostly present in the form of triacylglycerol (TG), consisting of a glycerol backbone and three long-chain fatty acids (LCFA) (2). Digestion and absorption of dietary fat is a highly efficient process, in which over 95% of ingested lipid is assimilated by human adults (3). However, because of their hydrophobic nature in an aqueous environment, lipid digestion and absorption are complicated processes. The assimilation process of lipid includes: a) mechanical emulsification, b) enzymatic hydrolysis, c) micellar formation with bile salts, d) absorption into the absorptive enterocyte, e) reesterification and packaging into chylomicrons and f) secretion into the circulation.

Free fatty acids (FA) and *sn*-2-monoacylglycerol (*sn*-2-MG) are the major digestive products of TG, mostly by the action of pancreatic lipase in the small intestine lumen. The small intestine cells possess two pathways for TG reesterification: the glycerol-3-phosphate pathway and the monoacylglycerol acyltransferase (MGAT) pathway. However, it is reported that TG is predominantly resynthesized via the MGAT pathway in the small intestine under physiological conditions (2). Despite its significant contribution to lipid assimilation in the enterocyte, detailed mechanisms are not fully elucidated. For example, identification of two different diacylglycerol acyltransferase (DGAT) isoforms (DGAT1 and 2) suggested the possibility that there may be distinct DGAT channels for the GPAT pathway and MGAT pathway (4). The exact function of MGAT in TG formation is also not completely understood. This study will focus on the influence of MGAT expression on metabolic utilization of fatty acids (FA) and monoacylglycerol (MG) in the cell.

Chapter II. Literature Review

2.1. Anatomy of the small intestine

The gastrointestinal tract is a hollow tube which has open ends at the mouth and anus, and passes through human body. The small intestine is the longest and most convoluted section with approximately 2.5~3 cm in diameter and 3~7 meters in length, which begins from the pyloric sphincter, and ends at the ileocecal valve (5,6).

The wall of this 7 meters long tube is composed of following 4 layers: serosa, muscularis propria, submucosa, and mucosa (Fig 1-1). The mucosa is further categorized into muscularis mucosa, lamina propria, and a single layer of epithelium which faces the lumen of the intestine (7,5). The epithelial cells, a fragile barrier between the body and the outside world, are distinguishable by their functions: absorptive epithelial cells, goblet cells, enteroendocrine cells, and Paneth cells (8).

The small intestine is where most of the digestion and absorption of nutrients occur, and has unique adaptation to facilitate these processes (7,9). One of the key characteristics of the small intestine is the surface complexity of the inner lining by folding of mucosa, finger-like projection of villi, and microvilli. This structural feature amplifies the surface area up to 600 fold, compared to the surface area of pipe having same diameter and length as the small intestine (9).

Following this general review, the highly polarized structure of the small intestine will be reviewed in terms of a) proximal to distal organization b) crypt to villus organization c) apical to basal organization of the enterocyte.

2.1.1. Proximal to distal organization

The small intestine gradually diminishes in diameter from proximal to distal, and it is divisible into three sections: the duodenum, the jejunum, and the ileum (10,5).

The duodenum is the shortest and the widest part of the small intestine. It is approximately 25 cm long, and receives the chyme from the stomach (5). Ducts that empty into the upper duodenum (sphincter of Oddi) deliver secretions from the pancreas and gallbladder (9).

The middle section of the small intestine, the jejunum is about 2.5 m long. There is no morphological distinction between jejunum and ileum; however the character of the small intestine is changed gradually, so that microscopically they show marked differences (5). Although the entire small intestine is available to take up digested nutrients, most of the absorption occurs in the jejunum (9).

The ileum is the distal section of the small intestine, and is approximately 3.5m long (5). When the chyme containing nutrients such as long chain fatty acids reaches the ileum, gastrointestinal hormones are released to signal satiety. The recycling of bile salts occurs by re-absorption in lower ileum (9).

Typically, digestion and absorption of nutrients is completed within the first 20% of the small intestine, before chyme reaches the ileum. Expression of the important enzymes related to uptake and reesterification of dietary lipids shows a proximal to distal gradient; plasma membrane long-chain fatty acid transport protein, FAT/CD36 (11), the small intestinal fatty acid binding proteins (I-FABP and L-FABP) (12), monoacylglycerol acyltransferase 2 (MGAT2) (13), and diacylglycerol acyltransferase 1 (DGAT1) (14) are reported to be dominantly expressed in the proximal and middle region, which is consistent with the lipid absorption pattern of gut.

Figure 1-1.

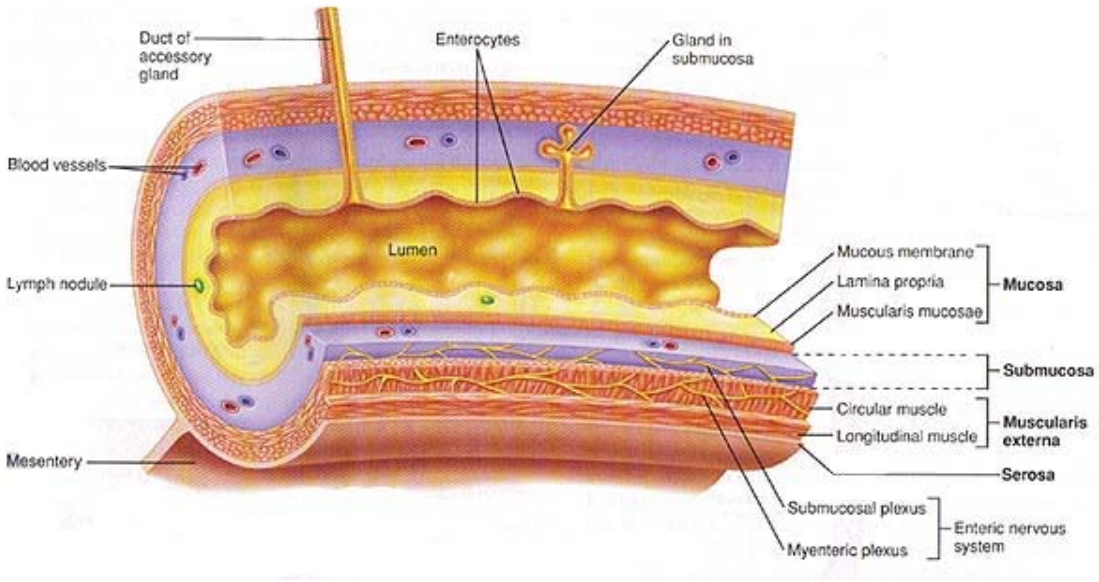

Figure 1-1. Anatomy of the small intestine (General structure of gastrointestinal wall) From Stanfield CL, Germann WJ (3)

Figure 1-2.

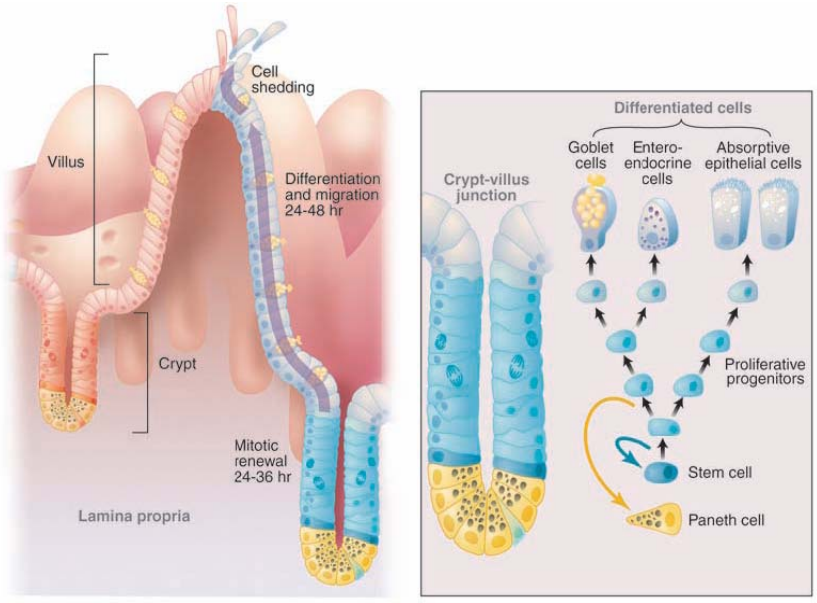

Figure 1-2. Anatomy of the small intestine (Crypt to villus organization) From Radtke F, Clevers H. (4)

Figure 1-3.

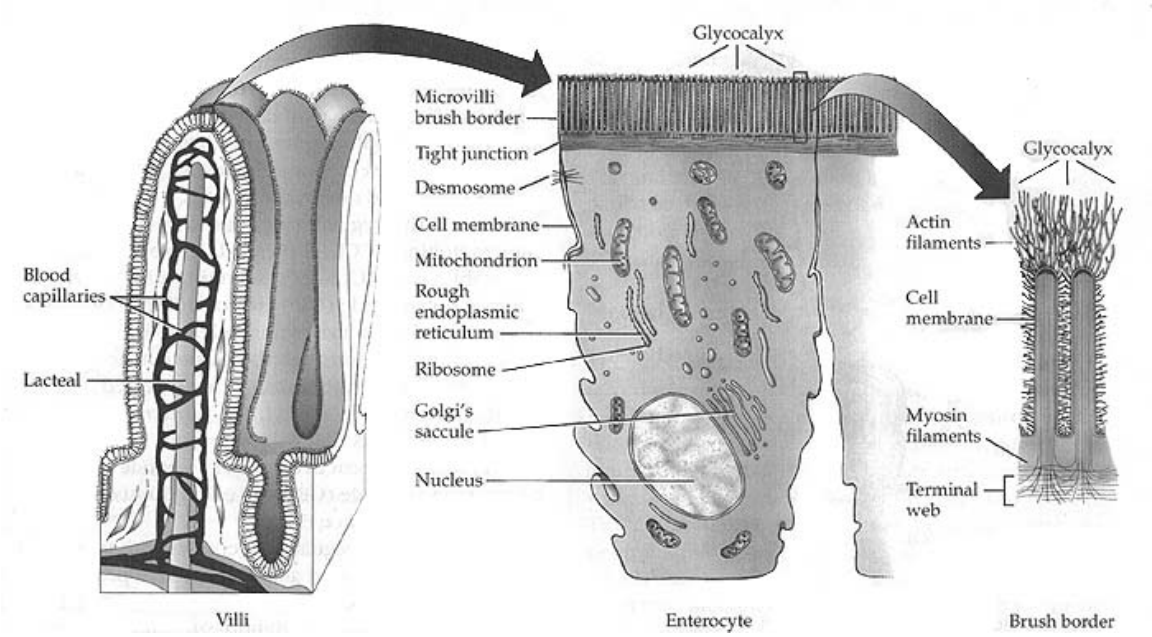

Figure 1-3. Anatomy of the small intestine (Apical to Basal organization of the enterocyte)

From Groff JL, Gropper SAS. (18)

2.1.2. Crypt to villus organization

The wall of the small intestine, the barrier against the outer environment, is composed of a single delicate layer of epithelium which has a well defined organization with continuous cell proliferation and loss to maintain homeostasis (8,15). Up to 70 billion cells are replaced per day in the adult intestine (1,8). This wall has velvet like appearance that is made of distinct crypt-villus units (5). The crypts (crypts of Lieberkühn) are mucosal invaginations where renewal of small intestinal cells takes place (16,17). The villi are fingerlike projections which extend the surface area of the small intestine for the efficient uptake of nutrients (Fig 1-2).

The crypts contain multi-potential stem cells which provide two main lineages: the absorptive lineage and the secretory lineage (8). The secretory lineages cover goblet cells secreting protective mucins, enteroendocrine cells secreting hormones, and Paneth cells controlling the microbial contents by secretion of antimicrobial agents (8). The enterocytes belong to the absorptive cells, represent 99% of total intestinal epithelial cells, and function to absorb nutrients. All of these cells differentiate during the migration along the crypt to villus axis, except Paneth cells which reside at the crypt bottom (Figure 1-2). It takes 2~5 days for cells to move from the crypt to the tip of villus, where cells are removed by apoptosis and exfoliation (17).

As enterocytes mature and migrate toward the villus, their morphological and functional characteristics change. Morphologically, the absorptive cells acquire more cytoplasmic organelles; endoplasmic reticulum (ER) becomes abundant, and Golgi complex further grows. Cell membranes also become highly organized with taller microvilli, thicker glycocalyx, and less permeable tight junctions (18). Functionally, the development of fatty acid esterification capacity is greatly enhanced during enterocyte differentiation (5). Moreover fatty acid esterification to TG shows longitudinal gradients throughout the crypt to villus, indicating that enzyme activities for TG synthesis are concentrated in the villus where most of nutrient absorption occurs (19). In

constrast, phospholipid (PL) synthesis enzymes are equally distributed along the crypt to villus unit (20). Lipid metabolism in the absorptive enterocytes will be discussed below.

2.1.3. Apical to basal organization of the enterocyte

The enterocytes are highly polarized, tall columnar epithelial cells with a general structure similar to other polarized epithelial cells; they have distinct surface membrane domains, and junctional complexes between cells (21) (Fig 1-3). In this absorptive epithelial cell are typical cellular components such as ER, Golgi complex, mitochondria, lysosomes, peroxisomes and other organelles throughout the cytoplasm. The nucleus usually resides near the basolateral membrane of the enterocyte (18).

After digestion in the small intestinal lumen, nutrients are absorbed across the apical membrane (AP) of the enteroctye, metabolized intracellularly, secreted across the basolateral membrane (BL) into the lymphatic or portal circulation, and transported to distant tissues. In order to accommodate remarkable capacity for the digestion and absorption of nutrients, the AP membrane has specialized adaptations which are distinct from those of the BL membrane.

The brush border consists of microvilli on the apical surface of the enterocyte, which number from 3000 ~ 6000 per cell (7) (Fig 1-3). These hair-like projections amplify the AP surface area, so that the absorptive efficiency of the gut is significantly increased. Some intestinal digestive enzymes, mainly disaccharidases and peptidases, are located on the brush border membrane, allowing for partial hydrolysis of digested nutrients before absorption (16,22-24). Structurally, these enzymes are glycoproteins, and their carbohydrate side chains may, in part, form a thick glycocalyx lining the luminal side of the intestine (20,24). The glycocalyx protects the epithelial cells in the gut from pancreatic digestive enzymes (25). This surface coat traps the water mixed with mucin secreted by Goblet cells, and creates an unstirred water layer (UWL) (9).

The lateral membrane possesses an intercellular junctional complex which maintains the structural integrity of the monolayer, and which forms a barricade to protect the body from the outside world: tight junction (zonular occludens), intermediate junction (zonula adherens), and desmosomes (macular adherens). The tight junction is located just below the brush border membrane, and seals the intercellular compartment from the luminal environment (2). It functions to maintain polarized morphology with distinct AP and BL domains, and to regulate paracellular diffusion of fluid and solute (21).

The characteristics of surface membranes determine the specialized functions of each domain in enterocytes (21). The basolateral membrane faces the extracellular fluid space, and has distinct structural and biochemical differences compared to those of the AP membrane, which faces the exterior of the body, suggesting specialized functions in cell survival and transport processes of nutrients. For example, the protein and glycoprotein patterns dominant in the BL membrane show significant differences from those in the AP domain (26,27). In addition, the protein to lipid ratio in the BL membrane is three times lower, and the cholesterol to phospholipid ratio is 20% lower compared to the AP membrane (16). The saturation of free fatty acid residues in PL in BL membrane is lower. Altogether, these compositional differences account for greater fluidity of the BL membrane than the AP membrane (28).

In addition, metabolic compartmentation between AP and BL domains of the enterocyte has also been reported. Apically absorbed long chain fatty acids and *sn*-2-MG are dominantly incorporated into TG, however, basolaterally provided fatty acids and MG are metabolized to PL or become oxidized (29-33). This metabolic polarity suggests the existence of different intracellular metabolic channels within the enterocyte.

2.2. Lipid digestion

Lipids in the typical Western diet are composed of TG, PL, free cholesterol and cholesterol ester (CE), and fat soluble vitamins (A, D, E and K). More than 90% of lipids consumed in the diet are TG, which are mainly esterified with LCFA (2).

The digestion of TG begins in the stomach by the action of gastric lipase, digesting ~30% of ingested TG (34). Partially hydrolyzed lipids enter the duodenum, and are completely digested by the combined actions of bile solubilization and pancreatic lipase hydrolysis, releasing fatty acids and *sn*-2-MG (2). Phospatidylcholine (PC), the major form of dietary and secretory PL, is broken down into fatty acid and lyso-PC by the pancreatic enzyme phospholipase A_2, which is activated by trypsin within the lumen of the small intestine (2). Most ingested cholesterol is present as free cholesterol, which is absorbed by the intestine. However 10-15 % of dietary cholesterol is present as the ester form, and hydrolyzed to fatty acid and free cholesterol by cholesterol esterase, also named carboxyl ester hydrolase or bile salt-stimulated lipase (35).

These digestion products are emulsified and form micelles with the help of bile salt and PC, which provides mechanisms for promoting absorption into the enterocytes by increasing surface area, and overcoming the UWL (2). The major enzymes involved in luminal TG hydrolysis will be briefly reviewed.

2.2.1. Gastric lipase

Dietary TG digestion begins with the action of gastric lipase secreted by chief cells in the stomach. Gastric lipase is also called acid lipase because its highest activity ranges in pH 4.0 to 4.5 (36). Gastric lipase accounts for the limited digestion of TG, estimated to be $\leq$ 30%, and acts preferentially on TG containing short- and medium- chain fatty acids (2).

It cleaves fatty acid at the *sn*-3 position of the TG at a rate that is twice as fast as that at *sn*-1 position, predominantly releasing fatty acid and 1,2-diacylglycerol (DG) (36). These features make gastric lipase particularly important for digestion of milk fat that consists of abundantly short- and medium- chain fatty acids in the *sn*-3 position (37). Although most of TG hydrolysis by gastric lipase occurs in the acidic environment, it is still active in the upper duodenum where the pH is 6 to 7 (2). However, the enzyme is inactivated by the action of pancreatic trypsin in the proximal small intestine, and further hydrolysis is completed by pancreatic lipase that is secreted into the lumen of the small intestine (36).

2.2.2. Pancreatic lipase

Pancreatic lipases are synthesized by the exocrine pancreas and subcategorized into 3 groups: a) pancreatic TG lipase (PTL), also called classical pancreatic lipase, b) pancreatic lipase related protein 1 (PLRP1), and c) pancreatic lipase related protein 2 (PLRP2). PTL preferentially hydrolyzes TG over PL and CE; therefore, most of the digestion of TG, especially those containing long-chain fatty acids, is carried out by PTL in the lumen of the upper small intestine. PLRP1 has no significant activity on lipid digestion, and the function of this protein is still obscure (38). On the other hand, PLRP2, which displays lipolytic activity, is believed to act as a critical enzyme for the digestion of dietary lipids in suckling animals (38,39).

PTL acts best at the water-oil interface, where the hydrolytic rate of the enzyme significantly increases when lipid concentrations exceed the limit of solubility, forming micelles (36). Bile salt, a physiological emulsifier, increases the total interface between the aqueous and the oil phases where PTL works. However, above the critical micellar concentration (CMC), bile salt interferes in the PTL activity by physical competition for the interface (2).

Under physiological conditions, this inhibitory effect of bile salt is overcome by a cofactor named colipase. This cofactor is synthesized by pancreatic acinar cells, secreted into the intestinal lumen, and activated by proteolytic cleavage of trypsin in the intestinal lumen (2,36). Colipase possesses distinct hydrophobic regions that are thought to act as a lipid binding site (37), and allows PTL to contact the bile salt-lipid mixture (2). PTL preferentially hydrolyzes fatty acids on the *sn*-1 and *sn*-3 positions of TG to release free fatty acids and *sn*-2-MG as the final products, which are absorbed by enterocytes (37).

2.2.3. Carboxyl ester lipase

Carboxyl ester lipase (CEL), also known as pancreatic cholesterol esterase or bile salt-stimulated lipase, has broad substrate specificity for CE, TG, PL, ceramide, and esters of vitamins A and D (2,40). The protein demonstrates nonspecific lipolytic activity, and catalyzes the hydrolysis of TG at all three ester linkages (36). A notable property of CEL is that *in vitro* it is able to hydrolyze *sn*-2-MG into fatty acid and glycerol, although it prefers *sn*-1-MG as a substrate (41). In the adult rat intestine, approximately 40% of *sn*-2-MG was reported to be completely hydrolyzed into glycerol and FFA before absorption, and this observation indirectly implies that CEL functions to degrade MG in the small intestine (42). The digestion of water-insoluble carboxyl esters with long chain fatty acids requires the activation of CEL by bile salt; whereas water-soluble carboxyl ester with short chain fatty acids are hydrolyzed by CEL in the absence of bile salts (40).

In the adult, it has been generally thought that CE hydrolysis is accomplished by CEL, and TG hydrolysis is achieved by the action of PTL. However, research with knockout (KO) mice suggests that lipid digestion is not so clearly defined. Net TG digestion and absorption was minimally influenced by the deficiency of PTL or CEL, but was significantly exacerbated in mice

lacking both enzymes (43-45), indicating their complementary function, and possibly suggesting involvement of other or yet unidentified lipolytic enzymes (44).

2.3. Uptake of FA and MG into the enterocyte

The brush border membrane (BBM) of enteroctyes is surrounded by an UWL which represents an important barrier for lipid uptake by enterocytes (2). The UWL is not mixed well with the bulk water of the intestinal lumen, so that molecules in the bulk water must cross this layer by diffusion before they are absorbed by enterocytes (46).The thickness of the UWL is considered to be rate limiting factor for intestinal absorption of lipids (47). Because the lipid digestion products, mainly fatty acids and *sn*-2-MG, are poorly dissolved in aqueous medium, only a few molecules are available to cross the UWL and gain access to the BBM (2,46).

To overcome the barrier, bile salts, which are biological detergents, allow formation of mixed micellar structure with lipolysis compounds, and significantly increase the concentration of lipid digestion products next to the BBM for effective absorption (2,46). The mechanism as to how fatty acids and *sn*-2-MG are taken up into enterocytes has been controversial. There are two suggested mechanisms for the uptake of fatty acids and *sn*-2-MG across the AP membrane of entercytes: a) passive diffusion, b) carrier-mediated uptake (46).

2.3.1. Passive diffusion

Once digested, lipids are in close proximity to the AP surface of enterocytes, these hydrophobic molecules may be able to diffuse freely through the lipids in the plasma membrane. The concentration gradient of lipids between the AP surface and the intracellular compartment initiates the diffusion into the enterocytes, and this concentration gradient is sustained by the

rapid reesterification of intracellular lipids into TG, allowing continuous diffusion into the cells (2).

Kamp *et al.* supported this idea by reporting the fast movement of un-ionized fatty acids across protein-free PL bilayers, suggesting that the diffusion process occurs spontaneously (48). In addition, Chow and Hollander demonstrated that at high concentrations of fatty acid, linoleic acid concentration and absorption showed a linear relationship, and the absorption rate was not influenced by the addition of metabolic inhibitors such as potassium cyanide or by decreasing the temperature from 37 to 20℃, supporting a passive diffusion mechanism (49).

2.3.2. Carrier-mediated uptake

The identification of membrane-associated fatty acid binding proteins on the AP surface of enterocytes introduced the concept that fatty acids may be taken up by a carrier-mediated transport system (50). This idea is supported by experiments showing that treatment of the intestinal membrane with trypsin or heat denaturation markedly decreased LCFA uptake (51,50). Moreover, Stremmel reported that absorption of radiolabeled oleate into rat intestinal cells showed saturation kinetics, with a lower K_m value compared to estimated monomer concentrations in the UWL, so that uptake into enterocytes occurs at maximum velocity (Vmax) (51). Overexpression of candidate fatty acid transporter proteins, such as fatty acid transport protein 4 (FATP4) located in the BBM of the enterocytes, in mammalian cells significantly enhanced the uptake of LCFA, also supporting a facilitated transport system (52,53). Kinetic data provide evidence that plots describing the relationship between LCFA concentration and LCFA uptake into intestinal cells show Michaelis-Menten fit or fit to a rectangular hyperbola when LCFA are at a low concentration, indicating a saturable function of concentration. On the other hand, at high concentrations of LCFA, uptake of LCFA revealed a linear relation to concentration,

suggesting that two different mechanisms are operable depending on the luminal concentration of fatty acids : 1) protein-mediated uptake at a low concentration of fatty acids, and 2) diffusion-mediated uptake at a high concentration of fatty acids (49,54,55).

Compared to extensive studies about fatty acid uptake across the cell membranes, there are very few studies concerning the absorption mechanism of *sn*-2-MG, the other major lipid digestion product. A kinetic study of *sn*-2-MG uptake across the apical surface of Caco-2 cells showed the saturable function of monomer concentration. Incubation of Caco-2 cells with trypsin before the MG transport experiment showed markedly reduced uptake of *sn*-2-MG, up to 40% (54), indicating the existence of a carrier-mediated transport process. However, diffusional absorption of MG into Caco-2 cells was detected at a high concentration of unbound MG, as well as the carrier-mediated absorption at a low concentration (55). These observations imply that depending on the concentration of monomer, *sn*-2-MG is taken up by either passive diffusion or facilitated transport, similar to the dual uptake mechanism of LCFA (46,49,55).

There are several candidate proteins considered to participate in LCFA uptake into enterocytes: plasma membrane fatty acid binding protein (FABPpm), FAT/CD36 (also named fatty acid translocase), and FATP4 (50,56,57). Absorption of [^{3}H] oleate and [^{3}H] monoolein into Caco-2 cells was significantly reduced by the addition of cold fatty acids or MG (54,55). This competitive inhibitory effect on fatty acid and MG uptake suggests that they share the same transport protein located on the BBM of enterocytes. Furthermore, the significant inhibition of monopalmitin uptake, as well as oleate uptake, after pretreatment of jejunal cells with anti-FABPpm indicated that these suspected proteins are also involved in the uptake of MG. (51). Drover *et al.* showed that CD36 was required to take up very long chain fatty acids (VLCFAs) in cultured cells, and the intestinal absorption of VLCFAs was completely blocked in CD36 null mice (58). Nonetheless, it remains unclear whether there are specialized membrane proteins which bind to lipid hydrolysis products to promote their transport into enterocytes (46).

In sum, both fatty acids and *sn*-2-MG appear to be taken up by concentration dependent dual uptake mechanisms, and at low monomer concentrations, they might use the same membrane proteins for carrier-mediated uptake into enterocytes.

2.4. Intracellular metabolism of FFA and MG

Following the uptake of lipid digestion products across the AP membrane of enterocytes, lipolysis products, largely FFA and *sn*-2-MG, are transported to the ER where the enzymes related to TG synthesis reside (2).

Two fatty acid binding proteins are highly expressed in the enterocyte, comprising approximaxtely 2 - 4% of total cytosolic protein (59): intestinal fatty acid binding protein (I-FABP) and liver fatty acid binding protein (L-FABP). These intracellular proteins have a clam-shell-like structure where ligands reversibly bind, and show high binding affinity for fatty acids, and other hydrophobic molecules (60). Compared to I-FABP binding of only fatty acids, L-FABP binds not only fatty acids but also other lipids such as lysophospholipids (LPC), *sn*-2-MG, retinoids, and bile salts, suggesting its involvement in intracellular MG transportation (59,61-63). Based on these observations, L- and I-FABP are thought to participate in the transporting and trafficking of FA and other lipolysis products in the aqueous environment of the cytosol (3,61).

Immunocytochemistry studies showed that staining for I- and L-FABP was stronger in the proximal intestine than the distal intestine, and in the villus cells rather than crypt cells. This expression gradient is consistent with the location at which most lipid digestion, absorption and metabolism take place (64). It is generally thought that both proteins are relevant to lipid metabolism in the epithelial cells of small intestine.

2.4.1. Anabolic process of MG and FFA toward TG synthesis

Sn-2-MG and FFA are reesterified to TG mainly in the ER, and this TG is packaged into chylomicrons (CM) with apolipoproteins such as B48 and A-IV, and are then carried to the BL membrane for secretion into the lymphatic circulation (2).

In the enterocyte, there are two biochemical pathways to synthesize TG: the glycerol 3-phosphate (G-3-P) pathway, and the monoacylglycerol acyltransferase (MGAT) pathway. As shown in Fig 1-4, the G-3-P pathway begins with acylation of G-3-P with a fatty acyl-CoA, yielding lysophosphatidic acid. This metabolic intermediate is further acylated and dephosphorylated to form *sn* -1,2-DG. The G-3-P pathway is a de novo pathway, and the enzymes relevant for this pathway are present in most tissues, including enterocytes (65,66). Another pathway to synthesize TG is the MGAT pathway, which initiates with reacylation of *sn*-2-MG with a fatty acyl-CoA by monoacylglycerol acyltransferase, yielding *sn*-1,2-DG. This pathway plays an important role for normal lipid absorption in enterocytes because significant amounts of *sn*-2-MG are released from dietary TG by the action of pancreatic lipase in the postprandial situation, and *sn*-2-MG acts as an inhibitor for the G-3-P pathway (67,68). It is thought that approximately 80% of TG incorporated into CM is resynthesized via the MGAT pathway after a meal (69,70). In both pathways, DG is finally acylated with fatty acyl-CoA to form TG by the action of diacylglycerol acyltransferase (DGAT) (66,71).

It is thought that three ER-localized MGAT enzymes (MGAT1, 2 and 3) are involved in the acylation of MG in the TG synthesis pathway (72-74). Although all three MGAT isoforms possess strong MGAT activities, only MGAT2 and 3 are considered to be directly involved in lipid metabolism in the enterocyte based on their tissue expression patterns: MGAT1 is highly expressed in stomach, kidney and adipose tissue, but not small intestine. Only MGAT2 and 3 are highly expressed in the small intestine. (75-78).

Figure 1-4.

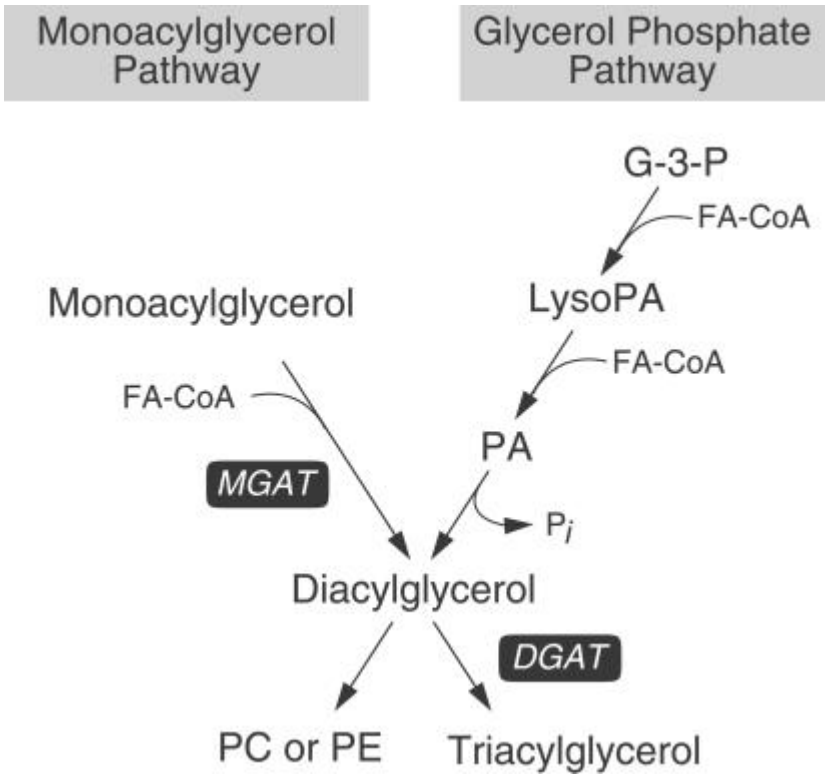

Figure 1-4. Simplified diagram for metabolic pathways of TG synthesis in the enterocyte. In the monoacylglycerol pathway, MGAT produces diacylglycerol, the precursor of triacylglycerol and certain phospholipids, by covalently joining a fatty acyl moiety to monoacylglycerol. In the glycerol phosphate pathway, diacylglycerol is derived from the dephosphorylation of phosphatidic acid (PA), which is produced by sequential acylation of glycerol 3-phosphate (G-3-P). FA-CoA, fatty acyl-CoA; LysoPA, lysophosphatidic acid; MGAT, MG acyltransferase2 in this case; P_i, inorganic phosphate; PC, phosphatidylcholine; PE, phosphatidylethanolamine. From Yen, *et al.* (74)

Between MGAT2 and MGAT3, MGAT2 is more likely to participate in TG resynthesis in enterocytes. Compared with MGAT3, which is mainly detected in the distal region of the small intestine, MGAT2 is highly expressed in the proximal part of the small intestine where dietary lipid digestion and absorption predominantly occur. Moreover the observation that expression of MGAT2, but not MGAT3, mRNA is up-regulated in mice fed high fat diets also supports an important role for MGAT2 in lipid uptake by the small intestine (72). Mice deficient in MGAT2 expression fully took up an ingested lipid load, but they had a delayed absorption rate. The intact lipid absorption in the intestine suggests that TG resynthesis in the MGAT null mice is mediated either by another MGAT enzyme which has not been identified yet, or by the G-3-P pathway, which is inefficient since breakdown of MG into glycerol and FA would have to occur first, requiring more energy than the MGAT pathway. It was suggested that delayed fat entry into the circulation raises the possibility of the dissociation of fat absorption from carbohydrate absorption and insulin secretion, which could direct the dietary lipid toward breakdown rather than ultimate storage in white adipose tissue (79).

As well as the MGAT activity, MGAT enzyme isoforms also possess DGAT activity in the order of MGAT3 > MGAT1 > MGAT2 (73). The location of MGAT2 gene nearby DGAT2 gene on the human chromosome 11 suggested that MGATs and DGAT2 might share a common ancestral gene (80). This hypothesis is further supported by the similar subcellular location of these enzymes, and higher sequence homology of DGAT2 with MGAT isoforms rather than DGAT1 enzymes (73).

Two DGAT enzymes, DGAT1 and 2, are detected in the enterocyte (71,81). DGAT1 belongs to the acyl CoA: cholesterol acyltransferase (ACAT)1 and 2 family (71). As mentioned above, DGAT2 is a member of an independent family of acyltransferases that includes MGAT1, 2, and 3 (81).

The topology of ER-associated enzymes relevant to TG synthesis provides important evidence about the process of lipoprotein packaging and TG storage in the enterocyte. Immunocytohistochemical studies demonstrated that the staining patterns of DGAT1 and DGAT2 were not completely merged, and that DGAT1 was more widely spread over the ER than DGAT2, reflecting the subcellularly separate locations of the two DGAT isoforms (73). This is consistent with previous studies in mouse liver, showing differences in enzymatic activities in liver microsomes. It was suggested that an overt DGAT, with catalytic residues residing on the cytosolic surface of the ER, plays an important role in the synthesis of TG pools stored in cytoplasm, whereas a latent DGAT, with catalytic residues residing on the luminal side of the ER, catalyzes synthesis of TG incorporated into VLDL (82,83).

Each DGAT is thought to have a distinct function based on unique biochemical and physiological characteristics. DGAT enzymes use not only DG as a substrate to synthesize TG, but also MG, though their catalytic properties are different: DGAT2 synthesizes TG from MG, but DGAT1 synthesizes TG or DG from MG, depending on substrate concentration (84). Moreover, compared with DGAT2, which recognizes only DG or MG as acyl acceptors, DGAT1 catalyzes acyltransferase reactions using acyl-CoA, and wax alcohol or retinol as substrates, as well as DG and MG, suggesting the involvement of DGAT1 in wax ester and retinol ester synthesis (85).

DGAT1 knockout mice survived and still synthesized TG, indicating compensation for the absence of DGAT1 by other enzymes in the enterocytes, such as DGAT2 and DG transacylase, which transfers a fatty acid moiety from one DG to another DG to synthesize TG (86-88). It was revealed that DGAT1 is not critical for TG absorption in the small intestine, but DGAT1 deficiency caused reduced chylomicron secretion and abnormal accumulation of lipid droplets in the enterocyte (86). In contrast, deletion of the DGAT2 enzyme caused more critical effects. DGAT2 knockout mice died shortly after birth due to impaired skin barrier function, and

this activity was not rescued by the activity of DGAT1, suggesting that DGAT1 and DGAT2 function differently in TG metabolism (89).

2.4.2. Catabolic process and MGL expression in the enterocyte

Although dietary lipid metabolism in the small intestine generally refers to the anabolic process of TG reconstitution mainly by the MGAT pathway, hydrolytic activities toward carboxylic acid esters were reported, and partial purification of MG hydrolyzing activity in the rat intestine suggested the presence of catabolic process in the enterocyte, and perhaps a specific activity for MG hydrolysis (90,91).

Monoacylglycerol lipase (MGL), a 32.9 kDa membrane-associated protein, is known to be involved in the complete degradation of intracellular TG in adipocytes and other tissues (92,93). Unlike other lipases such as hormone-sensitive lipase (HSL), which mainly hydrolyzes *sn*-1 or -3 ester bond of MG, MGL equally breaks down the *sn*-2 ester bond of MG as well as the *sn*-1 or 3 ester bonds (92,94). Therefore it is thought that MGL functions together with HSL to catalyze the hydrolysis of *sn*-2 MG, which is the hydrolysis product of HSL action on DG, and releases the FFA and glycerol into the adipocyte (93). In 1997, the MGL gene was cloned by the screening of a mouse adipocyte cDNA library, and the putative catalytic triad was identified. The MGL mRNA was detected in the various tissues, including adipose tissue, adrenal gland, ovary, heart, brain, spleen, lung, liver, skeletal muscle, kidney, and testis, but intestine was not tested (95).

The intestinal hydrolysis of MG was studied in Caco-2 cells, using radioactive *sn*-2-monoolein where the [^{3}H] label was on the fatty acid moiety (96). In this study, substantial radioactivity of *sn*-2-MG was recovered in the unesterified FA fraction, indicating possible degradation activity in Caco-2 cells. Experiments for the detection of MGL mRNA in Caco-2

cells and in rat small intestine confirmed the presence of MGL in the intestine (96,97). Significantly increased MGL expression and activity in mice fed high fat diets further supports a function for MGL in the assimilation of exogenous lipids (97), indicating the existence of a catabolic pathway as well as the major anabolic pathway in intestine.

In the present studies, the influence of MGAT2 on *sn*-2-MG and FFA metabolism in cells was investigated to understand the function of MGAT in TG synthesis. We tried to use Caco-2 cells since this cell line came from human intestinal epithelium, and had very weak MGAT activity compared with the intact enterocyte. However, due to inconsistent transfection experiment results, we changed the Caco-2 cells to CHO cells which are known to be easier for foreign cDNA transfection than Caco-2 cells, and we showed that they have no MGAT expression. Thus, through the over-expression of MGAT2 in cells, whose baseline TG synthesis occurs mainly via the G-3-P pathway, we expected to observe differences in TG synthesis between MGAT expressing cells and control cells, and to gain insight into the relative contribution of the MGAT and G-3-P pathways to TG synthesis. Therefore, the specific aims of the present study are:

1) Establishment of a transfection procedure to obtain the consistent expression of MGAT in a mammalian cell line with little or no baseline activity of MGAT.
2) Examination of the effects of MGAT expression on a) FA uptake b) MG utake c) FA metabolism and d) MG metabolism.

Chapter III. Materials and methods

3.1. Materials

[^{3}H] *sn*-2-Monoleoyl glycerol (glycerol-1,2,3-[^{3}H], 40 Ci/ mmol) was purchased from American Radiolabeled Chemicals, Inc (St. Louis, MO). [^{14}C] Oleoyl-CoA (oleoyl-1-[^{14}C], 57 mCi/mmol), and oleic acid (1-[^{14}C], 59.3 mCi/mmol) were purchased from PerkinElmer Life Sciences (Boston, MA). Unlabeled *sn*-2-monoolein and oleic acid were obtained from Doosan Serdary Research Laboratories (Toronto, Canada). Bovine serum albumin (BSA) (essentially free fatty acid free), oleoyl-CoA, Silica gel G thin layer chromatography (TLC) plates, ANTI-FLAG M2 monoclonal Antibody, Anti-Mouse IgG-Peroxidase antibody and protease inhibitor cocktail were obtained from Sigma Aldrich (St. Louis, MO). OctA-probe antibody to probe the FLAG-tagged proteins was purchased from Santa Cruz Biotechnology Inc. (Santa Cruz, CA). Anti-rabbit IgG-hoseradish peroxidase conjugate was obtained from Amersham Biosciences Inc. (Piscataway, NJ). The FLAG-tagged version of human MGAT2 cDNA was generously provided by Dr. Robert Farese (Gladstone Institue, San Francisco, CA). YM10 ultrafiltration membranes were purchased from Amicon Inc. (Beverly, MA). Dulbecco′s Modified Eagle′s Medium(DMEM), nonessential amino acids, trypsin-EDTA, F-12 media, pcDNA3(+), and Ligase T4 were obtained from Invitrogen (Carlsbad, CA). Fetal bovine serum (FBS) was from Life Technologies (Grand Island, NY). Fugene 6 Transfection reagent was purchased from Roche Diagnostics (Belleville, NJ). The Nucleofector I Device and Nucleofector Kits were purchased from Lonza, Inc. (Allendale, NJ).

3.2. Caco-2 cell culture

Caco-2 cells (American Type Culture Collection [ATCC], Manassas, VA) were cultured in Dulbecco′s modified eagle medium (DMEM) supplemented with 20% FBS, 1% multi

vitamins, and 1% nonessential amino acids in 5.0 % CO_2 atmosphere, and 100% humidity at 37 °C. The medium for Caco-2 cells was changed 3 times per week, and when cells reached 80~90% confluence, they were split with 0.25% trypsin-EDTA. The passage number for cells used for experiments was in between 25 and 43.

3.3. CHO-K1 cell culture

CHO-K1 cells (ATCC, Manassas, VA) were grown in F-12 Ham′s medium with 10% fetal bovine serum in 5.0% CO_2 atmosphere, and 100% humidity at 37 °C. The medium was changed 3 times per week, and cells were split with 0.25% trypsin-EDTA as they became 90% confluent. The passage number for cells used for experiments was in between 29 and 39.

3.4. Subcloning of hMGAT2 into pcDNA3.1 vector

For mammalian cell expression, the hMGAT2 cDNA was subcloned into the EcoR1 and Not1 sites of the pcDNA3.1/Hygro(+) vector. The hMGAT2 cDNAwas generously provided by Dr. Robert Farese (Gladstone Institue, San Francisco, CA). After ligation, sequences of the plasmid were analyzed by GENEWIZ, Inc. (Plainfield, NJ), and hMGAT2 sequences were confirmed by the sequence matching program provided by UC San Diego.

Mammalian cell expression

3.5. Expression of hMGAT2 in Caco-2 cells

Transient transfection was performed on Caco-2 cells with plasmid coding for hMGAT2. Cells were also transfected with a negative control empty vector without hMGAT2,

and a positive control vector which did not express hMGAT2 but instead expressed Green Fluorescence Protein. A positive control was used for checking the transfection efficiency, and an empty vector was used as the experimental control.

3.5.1. Liposome-based transfection using Fugene 6

3.5.1.1. 6 well culture dishes

Based on the optimized protocols established by the former investigator, Dr. Su-hyun Chon, 2.0×10^5 cells were plated per well in 6 well dishes (approximately 2.1×10^4 cells/ cm^2) (Day 0). On the next day, cells were transfected with a Fugene6 and hMGAT2 plasmid mixture at a 3 : 1 ratio of reagent (μl) to DNA (μg) (Day 1). Caco-2 cells were then incubated for up to 72 hr in a humidified incubator, and collected in ice-cold phosphate-buffered saline containing 0.5% (v/v) protease inhibitor cocktail (Day 2~4). Harvested cells were lysed using a Branson sonifier equipped with a microtip (Danbury, CT). MGAT assays were performed immediately to check the transfection efficiency, or cell lysates were stored at -70 ℃ for later use.

One set of the transfection experiments on 6 well dishes consisted of a non-transfected control well, a positive control well transfected with GFP, two negative controls transfected with empty vector, and two experimental samples transfected with hMGAT2. The relative MGAT activity was calculated by division of the MGAT activity in each hMGAT2-transfected sample into the averaged enzyme activity of the two negative empty vector controls.

3.5.1.2. Optimization experiment with 100 mm culture dishes

Caco-2 cells were plated into 100 mm dish at a density of 5.5×10^4 cells/ cm^2 (3.0×10^6 cells / dish), which was 50~60% confluent after 24 hr incubation (Day 0) (75,77). According to the manufacturer's recommendation, the transfection procedure was done using 3 : 2, 3 : 1 and 5 : 1 ratios of Fugene6 reagent (μl) to DNA (μg), respectively (Day 1). After 48 hr or 72 hr incubation, cells were collected as described above, and transfection efficiency was monitored by MGAT assays (Day 3~ 4).

3.5.1.2. 100 mm culture dishes

3.0×10^6 Caco-2 cells (5.5×10^4 cells/ cm^2) were seeded in 100 mm dish, a day before transfection (Day 0). Based on the optimization, transfection reagents and DNA mixture (approximately reagent (μl):DNA (μg) = 5 : 1) were added to plated cells (Day 1). 48 hr later, cells were harvested, and MGAT assay was performed to monitor gene expression efficiency (Day 2~3).

One set of transfection experiments using 100 mm dishes consisted of a non-transfected control, a positive control transfected with GFP, a negative control transfected with empty vector, and two or three experimental samples transfected with hMGAT2. The relative MGAT activity of each experimental sample was normalized to the MGAT activity of the empty vector-transfected control.

3.5.1.3. 100 mm culture dishes and FLAG-tagged hMGAT2 plasmid

hMGAT2 tagged with an N-terminal FLAG epitope (MGDYKDDDDV, epitope underlined) was expressed in Caco-2 cells as described above. Expression of FLAG-tagged

proteins was verified by both enzymatic assay for MGAT and Western blot analyses for FLAG (74,81).

3.5.2. Electroporation using Nucleofector Device

For the expression of hMGAT2 protein in Caco-2 cells, electroporation was performed using the Nucleofector device. Three negative controls were used: 1) the empty vector without hMGAT2 was used with application of the Nucleofector program for a comparison of MGAT activities. 2) hMGAT2 plasmid without application of the program was performed to assess the initial quality of cell culture and cell viability. 3) cells without any plasmids but with the application of the program were used to monitor the influence of the transfection of the plasmid DNA. As positive control, a vector containing Green Fluorescence Protein, but not hMGAT2, were used to monitor transfection efficiency, according to the manufacturer′s recommendation.

The number of Caco-2 cells was counted, and required amounts of cells (5.0×10^5cells/ well) were centrifuged at 90 × g, 4 ℃ for 10 min. After centrifugation, supernatant was discarded thoroughly, and the cell pellet was resuspended with Nucleofector solution T mixed with supplement solution provided by the company, to the final concentration of 5.0×10^5cells/ 100μl mixed Nuclefector solution T. To increase cell viability and transfection efficiency, the following transfection procedures were performed within 15 min after addition of the solution T to the cells: 2~4 μg (up to 10 μl) of DNA was added to 100 μl (5.0×10^5 cells) of Caco-2 cells and solution T mixture, and resuspended well. The sample was transferred to the cuvette provided in Nucleofector Kits. Then the cuvette was inserted into the cuvette holder of Nucleofector Device, and transfection program B-24 for Caco-2 cells was performed. To reduce the cell damage, pre-warmed 500 μl of RPMI medium was added to the cuvette after nucleofection, and then cells were carefully transferred to a 1.5 ml microcentrifuge tube using plastic pipettes included in the

Kits. For the recovery, cells were incubated at 37 °C for 10 min. After the recovery step, cells were seeded in the 6 well dishes and 3 ml of Caco-2 culture medium was added, and then incubated in 5.0 % CO_2 atmosphere, and 100% humidity at 37 °C for 24 hr~48 hr. Transfected cells were harvested in ice-cold PBS using cell scrapers, and were lysed by a sonifier equipped with a microtip. To monitor the transfection efficiency, MGAT assays were done immediately, or cell lysates were frozen at -70 °C.

The transfection experiment consisted of a positive control transfected with GFP, three negative controls with empty vector, and 1 ~ 3 hMGAT2-transfected samples. The MGAT activity of hMGAT2-transfected cells was divided by the average MGAT activity of the negative controls, and was expressed as relative activity.

3.6. Expression of hMGAT2 in CHO-K1 cells

CHO-K1 cells were used for transient transfection experiments with hMGAT2 plasmid DNAs. As a negative control, CHO cells were transfected with the empty vector that did not express hMGAT2, and as a positive control, separate vector encoding GFP was used. GFP expression was analyzed by fluorescence microscopy, and was used for checking transfection efficiency. An Empty vector was used as the experimental control.

3.6.1. Liposome-based transfection using Fugene 6

3.6.1.1. Optimization experiment in 100 mm culture dishes

24 hr before the transfection procedure was done, 2.0×10^6 ~ 3.0×10^6 cells of CHO-K1 cells (3.6×10^4 cells/ cm^2 ~ 5.5×10^4 cells/ cm^2) were plated in 100 mm dishes (Day 0). Based

on the manufacturer's recommendation, the transfection procedure was performed using 3 : 1 ~ 5 : 1 ratios of Fugene6 reagent (μl) to DNA (μg) (Day 1). After 48 hr, cells were harvested in ice-cold PBS by a cell scraper, and were lysed using a sonifier equipped with a microtip (Day 2~3). To monitor transfection efficiency, MGAT assays were done immediately, or cell homogenates were frozen at -70 °C.

3.6.1.2. 100 mm culture dishes

A day before transfection, CHO cells were plated at a density of 3.6×10^4 cells/ cm^2 (total 2.0×10^6 cells) in 100 mm dishes, resulting in ≤ 70 % confluence (Day 0). Cells were transfected with 11 μg of DNA with the 50.6 μl of Fugene6 based on the optimization experiments (Day 1). Two days after transfection (Day 2~3), CHO cells were harvested in ice-cold PBS with 0.5 % (v/v) of protease inhibitor, homogenized using a Branson sonifier, and MGAT assays were performed immediate, or the cell lysates were stored at -70 °C.

One set of transfection experiments was composed of a positive control transfected with GFP, a negative control transfected with empty vector, and 2~5 of hMGAT2-transfected samples. The MGAT activity of hMGAT2 expressing cells was normalized by the enzyme activity of the negative control transfected with empty vector in the same set.

3.6.1.3. 60 mm culture dishes

In order to reduce the amount of reagents used, transfection studies were performed in 60 mm dishes, according to the optimization experiments done with 100 mm dishes. CHO-K1 cells were maintained under the conditions described above.

3.6.1.4. Final experimental conditions

CHO-K1 cells were seeded at a density of 3.6×10^4 cells/ cm^2 (7.6×10^5 cells) in 60 mm dishes, resulting in ≤ 70 % of confluence (Day 0). After 24 hr incubation, seeded cells were transfected with mixture of 19.5 μl Fugene6 reagent and 4.2 μg DNA (4.6 : 1) (Day 1), and cultured in a humid incubator. Forty-eight hours after transfection (Day 2 ~ 3), cells were harvested in ice-cold PBS with 0.5 % (v/v) protease inhibitor cocktail by cell scrapers for the enzymatic assay. Collected cells were lysed for 30 sec using a Branson sonifier equipped with a microtip, and enzymatic assays were carried out immediately, or lysates were frozen at -70 °C before use.

The transfection experiment consisted of a positive control transfected with GFP, a negative control, and one to eight of hMGAT2-transfected samples. The MGAT activity of the hMGAT2 expressing sample was normalized by enzyme activity of the empty vector -transfected control.

3.7. In vitro assay for MGAT activity

In order to monitor the success of hMGAT2 DNA transfection into cells, the incorporation of [^{14}C] oleoyl-CoA into DG was measured. The MGAT assay was modified in the laboratory based on the method of Coleman and Haynes, as described by Chon, *et al*. (97,98)**.**

Harvested cell lysates were concentrated using YM10 ultrafiltration membranes, and protein concentration was determined by Bradford assay (99). 7~20 μg of lysate proteins were assayed for 10 min at 25 °C in a final volume of 200 μl using 25 μM mixture of [^{14}C] radiolabeled,

and unlabeled oleoyl-CoA, and 250 μM *sn*-2-monoolein as substrates. These conditions were shown previously to be linear for time and for protein concentration (100). The assay buffer contained 100 mM Tris-HCl, 4 mM $MgCl_2$, 1 mg/ml bovine serum albumin, and 100 μM each of phosphatidylcholine and phosphatidylserine. Reactions were initiated by adding [^{14}C] oleoyl-CoA, and terminated by placing reaction tubes on ice. Lipids were extracted using chloroform/methanol (2 : 1, v/v) and the organic phase was analyzed using thin layer chromatography (TLC) with hexane: ethyl ether: acetic acid (70 : 30 : 1. v/v/v). Quantification of each lipid fraction separated by TLC was analyzed using the Molecular Dynamics STORM scanner and ImageQuaNT software. MGAT activities of samples were calculated according to standard curves. To plot the standard curves, specific amounts of [^{14}C] oleate were spotted on the TLC plates.

3.8. Western blot analysis of protein expression

For a pilot study of western blot analysis, Caco-2 cells in which the MGAT-transfection efficiency was confirmed by enzyme assay were used. Cells were homogenized with a Branson sonifier equipped with a microtip (Danbury, CT), and stored at -70 °C before use. The cell lysates were concentrated using YM10 ultrafiltration membranes at 5,000 × g for 1hr at 4 °C.

Concentrated Caco-2 cell homogenates were denatured by boiling in SDS-loading buffer having 2% 2-mercaptoethanol for 5 min. 40~50ug of proteins were loaded onto 9% polyacrylamide gels and seperated by SDS. The proteins were transferred to nitrocellulose membranes by semi-dry transfer system (BioRad) for 1~1.5 hr at 15~20 V. To prevent non-specific binding, the membranes were incubated in washing buffer containing 5% nonfat milk, at 4 °C overnight. Then the protein was probed with primary antibody for up to 2 hr at room temperature (OctA-Probe antibody, 1 : 300 and ANTI-FLAG M2 monoclonal antibody, 1 : 200 ~ 1 : 1000). After 3 washes, membranes were incubated with anti-rabbit IgG-hoseradish peroxidase

conjugate secondary antibody at 1 : 5,000 dilution for 1 hr at room temperature, or in case of using ANTI-FLAG M2 antibody, anti-mouse IgG-Peroxidase secondary antibody at 1 : 5000~1 : 10000 dilution for 1 hr at room temperature. Blots were developed using ECL reagent (GE Healthcare, Piscataway, NJ), and exposed to film (Kodak X-OMAT) for 30 sec up to 25 min. Homogenates of CHO cells stably transfected with FLAG-CD36 (provided by N. Abumrad) were used as a positive control.

3.9. Preparation of the radiolabeled FFA and MG media

For uptake and metabolism studies, 30 μM of radiolabeled oleic acid (18:1) or *sn*-2-monoolein (18:1) were dried under N_2, and dissolved in 0.5% of ethanol (volume to final volume) (101). The lipids were then dispersed in 100 μM of BSA (essentially fatty acid free, typical plasma albumin concentration) in F-12 medium without BSA at 37 °C for 1 hr with 90 rpm of shaking in a water bath. The unbound concentration of oleic acid and *sn*-2-monoolein bound to BSA were 0.02 μM, and 0.09 μM respectively (54).

3.10. Metabolism of [^{14}C] oleic acid and [^{3}H] *sn*-2-monoolein in CHO-K1 cells

The metabolic fates of radiolabeled oleic acid and *sn*-2-monoolein in CHO cells were examined. Transfection procedures were done as described above for CHO-K1 cells.

15 hours before starting experiments, the media were replaced with serum free F-12 medium. At time 0, the cells were incubated with the prepared media containing BSA bound radiolabeled lipids for 2, 6, or 24 hour at 37 °C. At each time point, cells were harvested after washing with ice cold stop-solution (0.5% BSA- PBS) three times, and ice cold PBS three times. Every procedure was done on ice to stop further uptake and metabolism.

For uptake measurements, some of the collected cells were sonicated, total cell homogenates were solubilized in Ultrafluor (Fisher Scientifics, Pittsburgh, PA), and radioactivity was measured in a scintillation counter. Protein concentration was determined by Bradford assays (99).

Total cell lipids were extracted by the method of Bligh and Dyer (102). After extraction, the recovery of radioactivity was approximately 95% of that prior to lipid extraction. The incorporation of [^{14}C] oleic acid, and [^{3}H] *sn*-2-monoolein into lipid metabolites was determined by two-step thin layer chromatography (TLC) separation, as follows: in case of using [^{14}C] oleic acid, because [^{14}C] lipids could be visualized and quantified by the Dynamics STORM scanner and ImageQuaNT software, sample extracts only were spotted onto 20 × 20 cm TLC plates under N_2 gas. However, [^{3}H] labeled lipid extracts, which were impossible to detect with the scanner, were spotted onto plates with lipid standards (cholesterol oleate (CE), triolein (TG), oleate (FA), *sn*-1,2-diolein (DG), *sn*-2-monooleoin (MG), phosphatidylcholine(PC), and phosphatidylserine(PS)). All plates were developed to 6 cm height from the bottom of the plates in chloroform: methanol: acetic acid: formic acid: distilled water (35 : 15 : 6 : 2 : 1 v/v), and dried under the hood for 10 min. Subsequently, the plates were fully developed to 18 cm of the plates in hexane : ethyl ether : acetic acid (70 : 30: 1 v/v). As mention earlier, [^{14}C] labeled samples were visualized and quantified using the Dynamics STORM scanner and the ImageQuanNT software. [^{3}H] labeled metabolites were visualized by iodine vapor, and then the area corresponding to each lipid was marked, scraped and collected into 5 ml Ultrafluor. Radioactivity was determined using a scintillation counter.

3.11. Statistical methods

Data are presented as means ± S.E.M. Differences were analyzed by two-way analysis of variance at the $p < 0.05$ level.

Chapter IV. Results

4.1. hMGAT2 expressed in Caco-2 Cells

4.1.1. hMGAT2 expression in Caco-2 cells using the liposome-based transfection method and 6 well culture dishes

The human colorectal adenocarcinoma cell line Caco-2 was selected as the most relevant in vitro model to investigate the influence of hMGAT2 expression on intestinal FA and MG uptake and metabolism. Caco-2 cells have several functional characteristics similar to mature villus cells of the small intestinal epithelium, but they also have limitations, for instance, although Caco-2 cells have both G-3-P and MGAT pathways to synthesize TG, MGAT activity in Caco-2 cells is only 10% of enzyme activity of primary enterocytes. However, due to this limitation, Caco-2 cells are a desirable cell model system for our experiment, in which we wished to observe effects of MGAT expression on lipid metabolism.

For the expression of hMGAT2, Caco-2 cells were transiently transfected using the liposome-based transfection reagent, Fugene 6. The transfection procedure was as follows: 1) 24 hr before transfection, Caco-2 cells were seeded on 6 well plates. 2) Then plated cells were transfected with a mixture of Fugene6 and hMGAT2 cDNA at a 3 : 1 ratio of reagent to DNA. 3) 72 hr after transfection, when MGAT activity was expected to have reached the peak, cells were harvested in the ice-cold PBS. 4) The MGAT expression in the hMGAT2 transfected cells was monitored by MGAT activity assay.

Since *sn*-2-monoolein and [^{14}C] oleoyl-CoA were provided as substrates in the enzymatic assay, cells expressing hMGAT2 proteins should incorporate more radioactivity into DGs than controls transfected with the empty vector. In the MGAT assay, cells demonstrated weak radioactivity incorporation into TG as well as DG. Although it was reported that the MGAT2 enzyme possesses DGAT activity, the DGAT activity was much weaker when compared

Figure 2.

A. **B.**

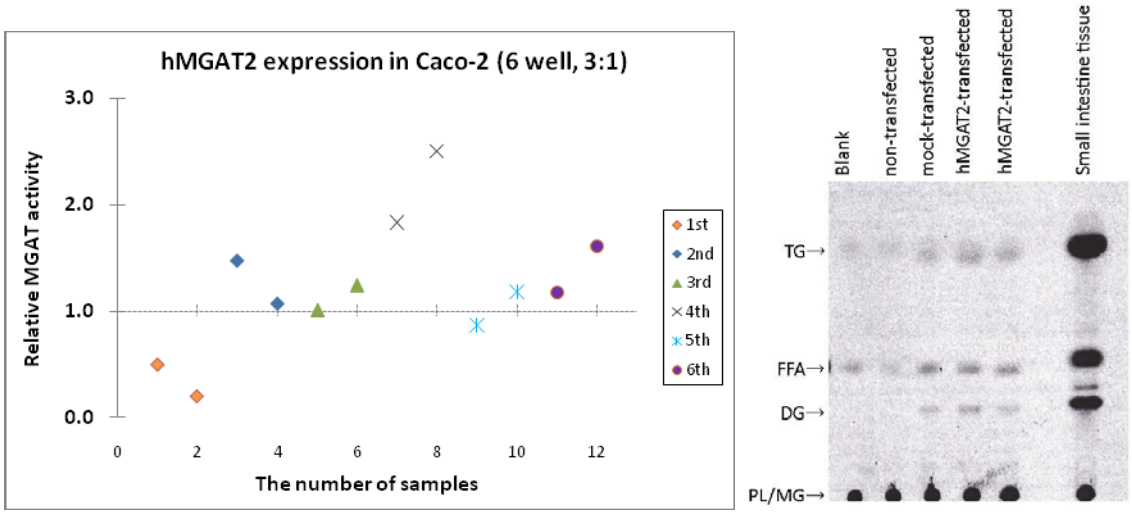

Figure 2. hMGAT2 expression in Caco-2 cells. ***A***, The relative MGAT activity of hMGAT2-transfected Caco-2 cells using Fugene6 (reagent (μl) : DNA (μg) = 3 : 1) and 6 well culture dishes. Each enzyme activity is calculated as described in "Materials and Methods," and results are expressed relative to empty vector-transfected controls in each separate experimental set. n = 12, total 6 sets of transfection experiments. ***B***, Representative result of the MGAT assay with samples using Fugene6 (reagent (μl) : DNA (μg) = 3:1) and 6 well culture dishes. For the assay, 7 μg of cell lysate protein was used.

with MGAT activity in the assay (75), and Yen *et al*. demonstrated substrate specificity of hMGAT2 toward MG as a fatty acyl group acceptor (77). Thus, it was considered that some portion of DG, the end product of hMGAT2, was further esterified to TG by the action of endogenous DGAT activity in the cells (77). The TG, which consisted of one MG and potentially two radiolabeled oleates, could have twice the radioactivity signal, so that a half of the radioactivity counts in TG also counted as MGAT activity (97).

Under the experimental conditions described above, Caco-2 cells transfected with hMGAT2 demonstrated inconsistent MGAT activities. Some hMGAT2-transfected cells showed clear radioactive signals in DG and TG spots, however, other hMGAT2-transfected cells showed no significant differences when compared to controls transfected with empty vector (Fig 2-B). Moreover, as shown in Fig 2-A, even though cells showed MGAT activity, the levels were not significantly higher (at most 2.5-fold) than empty vector-transfected controls. In conclusion, MGAT expression in Caco-2 cells was not consistent with this transfection condition. Therefore, the experimental results could not be trusted, since it could not necessarily be said that any positive results were definitely the effects of MGAT protein expression.

4.1.2. hMGAT2 expression in Caco-2 Cells using the liposome-based transfection method and 100 mm culture dishes

Optimization experiments were performed based on published papers reporting successful expression of MGAT in Caco-2 cells or other mammalian cells (75,77). In both papers, researchers used 100 mm culture dishes for the transfection experiments. As the growth rates and distribution of cells on 6 well plates and 100 mm dishes were compared by seeding the same

Figure 3.

A. **B.**

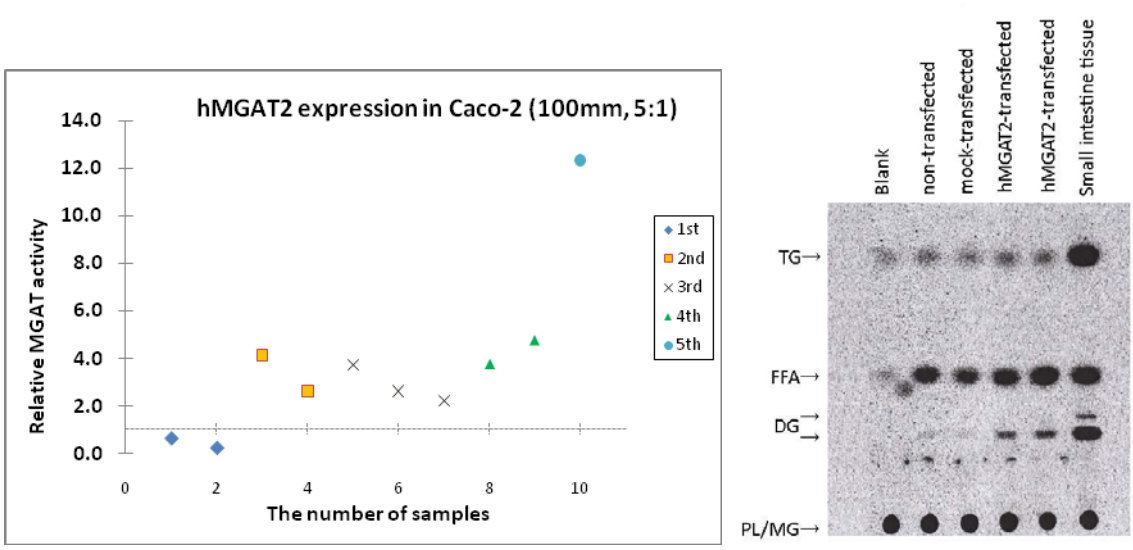

Figure 3. hMGAT2 expression in Caco-2 cells ***A***, The relative MGAT activity of hMGAT2-transfected Caco-2 cells using Fugene6 (reagent (μl) : DNA (μg) = 5 : 1) and 100 mm dishes. Each enzyme activity is calculated as described in "Materials and Methods," and results are expressed relative to empty vector-transfected controls in each separate experimental set. n = 10, total 5 sets of transfection experiments. ***B***, Representative result image of MGAT assay with samples using Fugene6 (reagent (μl) : DNA (μg) = 5:1) and 100 mm dishes. For the assay, 20 μg of cell lysate protein was used.

relative density of cells, we found that cells in 100 mm dishes showed a relatively slower growth rate and equal distribution. We assume that the differences were caused by the small dimension and slightly convex surface of the 6 well plate compared with the 100 mm dish.

After we decided to use 100 mm dishes for transfection experiments, optimization experiments were performed. In optimization experiments for 100 mm dishes, the cell number seeded onto plates, ratio of Fugene6 to DNA, and incubation times after transfection were varied, since both papers (75,77) gave only rough numbers for those factors (results not shown). The tranfection procedure using 100 mm dishes was as follows: 1) Caco-2 cells were plated in 100 mm dishes a day before transfection at 3.0×10^6 cells / dish, 2) and then transiently transfected with a Fugene6 and hMGAT2 plasmid mixture at approximately a 5 : 1 ratio of reagent to DNA. 3) After 48 hr incubation, cells were collected in ice-cold PBS, 4) and the expression of the targeted protein was monitored by MGAT assay. In the enzyme assay using [^{14}C] oleoyl-CoA as the radiolabeled acyl donor, Caco-2 cells expressing hMGAT2 were found to incorporate significantly higher amounts of radioactivity into DG than control cells transfected with empty vector without hMGAT2 (Fig 3-B). Slightly higher radioactivity was also detected in TG in hMGAT2 expressing cells compared to controls. The MGAT activity of hMGAT2-transfected Caco-2 cells was up to 12-fold higher than that of control-transfected cells (Fig 3-A) although the averaged relative MGAT activity was 3.7 ± 1.1.

Although under this condition, the transfection efficiency was much more consistent compared to previous trials using 6 well plates and 3 : 1 ratio of Fugene6 to DNA (Fig 2-A), nevertheless, the degree of MGAT activity was still variable. Moreover, there were still exceptions of cells for which there was no increase in MGAT activity (Fig 3-A). Therefore, it was decided that FA and MG metabolism studies could not be performed under this transfection condition due to uncertain reliability of the MGAT transfection efficiency.

4.1.3. FLAG-tagged hMGAT2 expression in Caco-2 cells using the liposome-based transfection method and 100 mm culture dishes

Even though the transfection efficiency of Caco-2 cells was relatively improved after the experiment had been performed using the larger culture dishes, optimized cell density, and optimized ratio of Fugene6 to DNA, the expression of hMGAT2 in cells was not 100 % reliable. To compensate for the instability of the transfection, we attempted to use FLAG-tagged plasmids, so that Western blot analysis could be used to detect the expression of hMGAT2 proteins by an anti-FLAG antibody. The samples could then be used to directly examine FA and MG metabolism using the detection of radioactivity.

In order to confirm the reliability of the Western blot analysis, pilot studies were conducted with cell lysates whose expression of the protein was proved by the MGAT assay. In these samples, FLAG-tagged hMGAT2 proteins should be detected with molecular mass of ~33 kDa by Western analysis. As we performed Western blots with OctA-Prove primary antibody for the detection of FLAG-tagged proteins (Santa Cruz Biotechnology Inc., Santa Cruz, CA), the positive control, CD36-FLAG, was detected, however, no signal for MGAT-FLAG was observed (Fig 4-A). Based on information that Dr. Eric Yen, who had performed immunoblotting analysis with the FLAG-tagged hMGAT2 (103), kindly provided, Western blot analysis was also conducted using the ANTI-FLAG M2 antibody (Sigma Aldrich, St. Louis, MO), but only non-specific bands were detected, as shown in Fig 4-B, even for the positive control. In short, although the expression of hMGAT2 was confirmed by MGAT assay, the expected ~33 kDa protein was not detected by Western blot analysis with the same antibodies that had successfully detected FLAG-tagged hMGAT2 protein previously.

Figure 4.

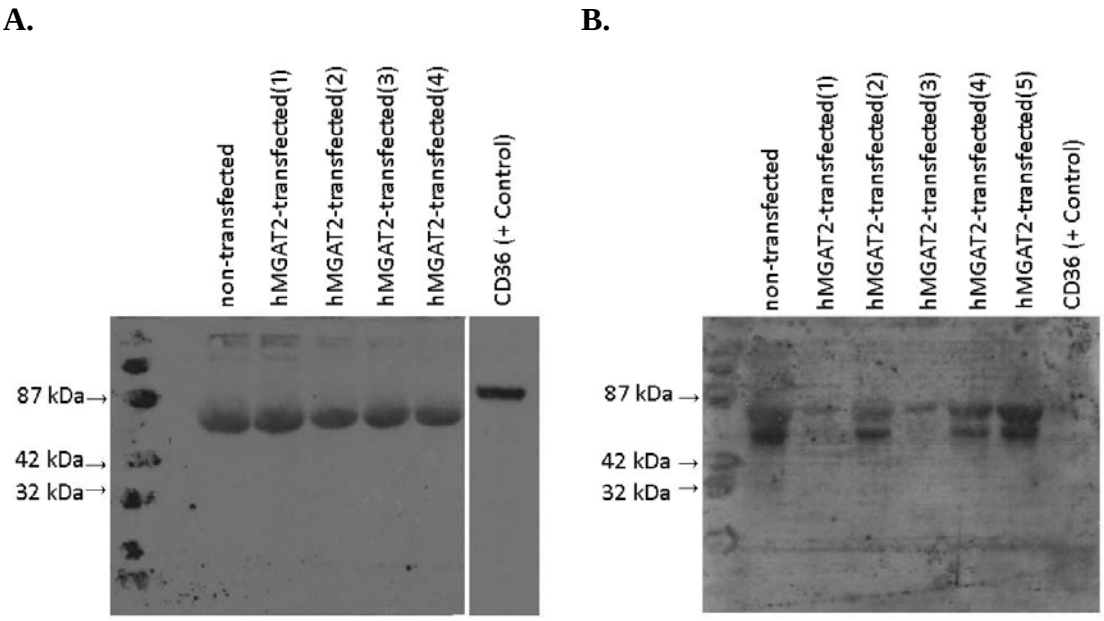

Figure 4. FLAG-tagged hMGAT2 expression in Caco-2 cells. ***A***, Representative result of Western blot analysis using Oct-A Prove antibody. 50 µg of Caco-2 cell homogenates were probed with OctA-Probe anti-FLAG primary antibody (1:300) and anti-rabbit IgG-horseradish peroxidase conjugate second antibody (1:5000). FLAG-tagged CD36 (~87kDa) was used as a positive control. CD36 is from CHO cells. ***B***, Representative result of Western blot analysis using ANTI-FLAG M2 antibody. 50 ~ 40 µg of Caco-2 cell homogenates were probed by ANTI-FLAG M2 monoclonal primary antibody (1:500) and by anti-mouse IgG-peroxidase second antibody (1:2000). FLAG-tagged CD36 (~87kDa) was used for a positive control. CD36 is from CHO cells.

Before performing the pilot study, FLAG-tagged sequences of hMGAT2 plasmids were checked, and it was found that the FLAG sequence was changed from DYKDDDD**G** to DYKDDDD**V**. Thus, we questioned the reliability of using ANTI-FLAG M2 antibody known to detect DYKDDDD**G**, and asked technical support in Sigma about this anti-FLAG antibody. They replied that the antibody would work because it recognized and bound to DYKDDD sequences. Nonetheless, as mentioned previously, ANTI-FLAG M2 antibody did not detect the expected protein. It is possible that the unexpected change in the FLAG sequence caused this result, or that the amount of FLAG-hMGAT2 protein was insufficient for detection despite being adequate for the MGAT activity assay which was likely a more sensitive method to detect hMGAT2 proteins. Unfortunately, therefore, we were not able to use the FLAG tag as a measure of hMGAT2 transfection efficiency.

4.1.4. hMGAT2 expression in Caco-2 cells using the electroporation method

Electroporation using the Nucleofector device (Lonza, Inc.,Allendale, NJ) was performed to improve reliability and to increase the transfection efficiency of hMGAT2 in Caco-2 cells. Based on the recommendations of the manufacturer, required amounts of cells were suspended with Nucleofector solution T and DNA. The mixture was transferred to the Nucleofector cuvettes included in the Nucleofector kits, and the designated program for Caco-2 was used. To increase cell viability, transfected cells were recovered in RPMI medium, and then seeded in 6 well dishes. After 24 hr ~ 48 hr incubation, cells were harvested and the expression of hMGAT2 protein was monitored by the enzyme assay.

Although electroporation is reported to be a more efficient way to introduce desired foreign DNA into cells compared to the liposome-based transfection methods, in the aspect of cell viability, this method was inappropriate for collecting enough cells to conduct the assay.

Figure 5.

A. **B.**

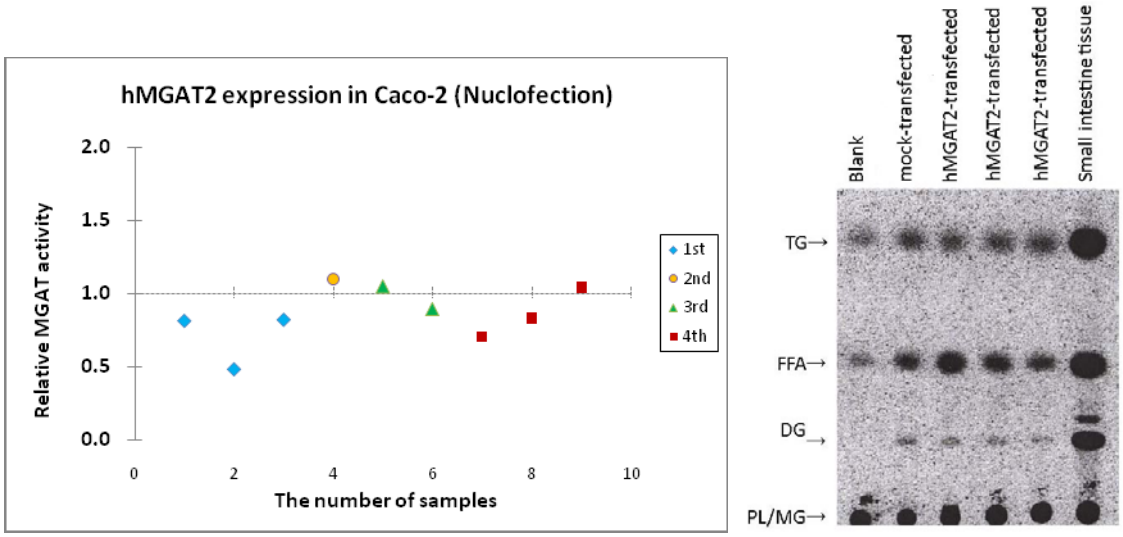

Figure 5. hMGAT2 expression in Caco-2 cells. ***A***, The relative MGAT activity of hMGAT2 transfected Caco-2 cells using Nucleofector devices and 6 well culture dishes. Each enzyme activity is calculated as described in "Material and Methods," and results are expressed relative to empty vector-transfected controls in each separate experimental set. n = 9, total 4 sets of transfection experiments. ***B***, Representative result of the MGAT assay with samples using Nucleofector and 6 well culture dishes. For the assay, 14 µg of cell lysate protein was used.

Moreover the MGAT assay results indicated that both MGAT-transfected samples and empty vector-transfected control samples incorporated similar amounts of radioactivity into DG. hMGAT2-transfected cells showed slightly higher incorporation into TG; there was, however, no significant difference from controls. This suggested that samples transfected with hMGAT2 by Nucleofector did not produce desired levels of MGAT proteins; therefore it would not be dependable to carry out the FA and MG metabolism studies in cells exposed to this transfection condition.

4.2. hMGAT2 Expressed in CHO-K1 Cells

4.2.1. hMGAT2 expression in CHO-K1 cells using the liposome-based transfection method and 100 mm culture dishes

The Caco-2 cell line was our desired cell model to investigate the influence of MGAT on enterocyte lipid metabolism, but, as described in the previous section, despite attempts to introduce hMGAT2 plasmids into Caco-2 cells using various methods and conditions, transfection efficiency was inconsistent at best. Thus, we decided to change the cell model to CHO-K1, which is a widely used cell model for the expression of foreign DNAs. To study the effect of MGAT expression on FA and MG uptake and metabolism, CHO-K1 cells were transiently transfected with hMGAT2 by the liposome-based method.

Based on optimization experiments (results not shown), CHO-K1 cells were transiently transfected with hMGAT2 DNA with Fugene 6 mixture (approximately reagent (μl) : DNA (μg) = 5 : 1). Then, the cells were collected after 48 hr incubation, as MGAT activity would be expected to have reached the peak, and the expression of hMGAT2 in CHO-K1 cells was analyzed by enzymatic assay for MGAT.

Figure 6.

A. **B.**

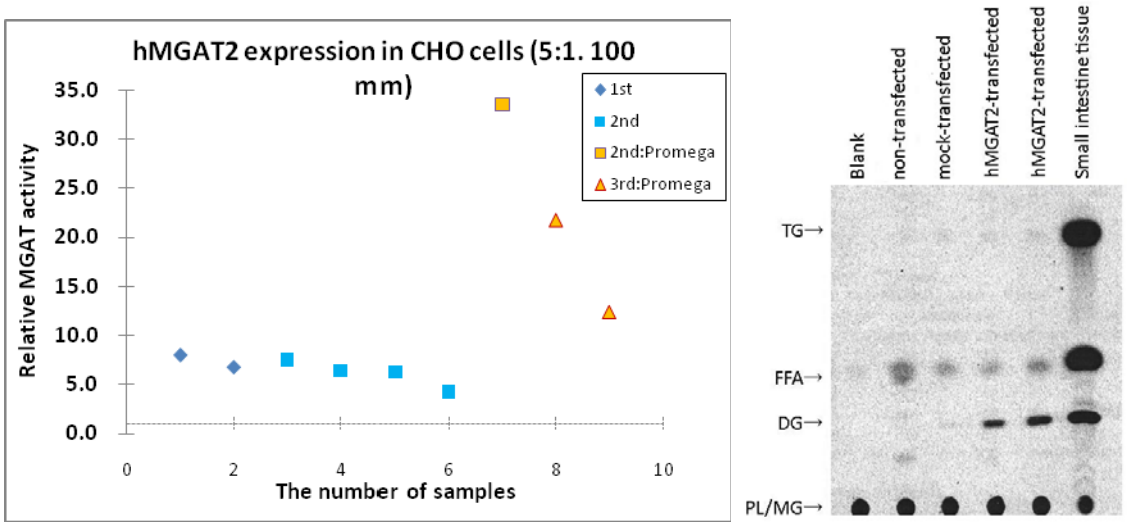

Figure 6. hMGAT2 expression in CHO-K1 cells. ***A***, The relative MGAT activity of hMGAT2-transfected CHO-K1 cells using Fugene6 (reagent (µl) : DNA (µg) = 5 : 1) and 100 mm dishes. Each enzyme activity is calculated as described in "Material and Methods," and results are expressed relative to empty vector-transfected controls in each separate experimental set. Blue dots represent the experiments using plasmid DNAs purified by EndoFree Maxi prep kits (Qiagen), and yellow dots are for the experiments using DNAs purified by PureYield plasmid prep kits (Promega) n = 6, and n=3 respectively. Total 3 sets of transfection experiments. ***B***, Representative result of MGAT assay with samples using Fugene6 (reagent (µl) : DNA (µg) = 5:1) and 100 mm dishes. For the assay, 20 µg of cell lysate protein was used.

The assay results demonstrated that CHO-K1 cells transfected with hMGAT2 cDNA incorporated significantly higher radiolabeled FA substrate (18:1) in DG, and slightly higher radiolabeled FA in TG than controls transfected with empty vector (Fig 6-B).The transfection efficiency in the CHO-K1 cells was quite consistent with 4.3 to 8.0-fold higher MGAT activity compared to empty vector-transfected control. Moreover, after we changed the plasmid DNA purification kits from EndoFree Plasmid Maxi (Qiagen Cat. # 12362) to PureYield Plasmid Miniprep (Promega, Cat. # A1223), the relative enzyme activity of hMGAT2 transfected cells was elevated even further, at least 12-fold and up to 33-fold higher than empty vector controls. Therefore, when the FA and MG uptake and metabolism study would be performed under this transfection condition with CHO-K1 cells, we were confident that any differences between experimental hMGAT2-transfected groups and empty vector-transfected control groups would be caused by the expression of MGAT.

4.2.2. hMGAT2 expression in CHO-K1 Cells using the liposome-based transfection method and 60 mm culture dishes

Although CHO-K1 cells transfected with hMGAT2 showed significant MGAT activity compared to empty vector-transfected controls, huge amounts of radioactive substrates must be used to provide sufficient volume of medium cover the monolayer of plated cells (at least 4 ml per 1 dish) in this experimental condition with 100 mm dishes. For safe and reasonably priced metabolism studies with radioactive chemicals, it was desirable to reduce the surface area of the cell monolayer using 60 mm dishes, and subsequently, the entire quantity of radiolabeled lipids for the experiments could be minimized.

According to the transfection experiments with 100 mm dishes, cell numbers to be seeded were determined to obtain the same cell density (3.6×10^4 cells/ cm^2), and then transfection experiments were performed following the optimized protocol with Fugene6. Transfection efficiency was monitored by MGAT assay. The enzymatic assay demonstrated that

Figure 7.

A. **B.**

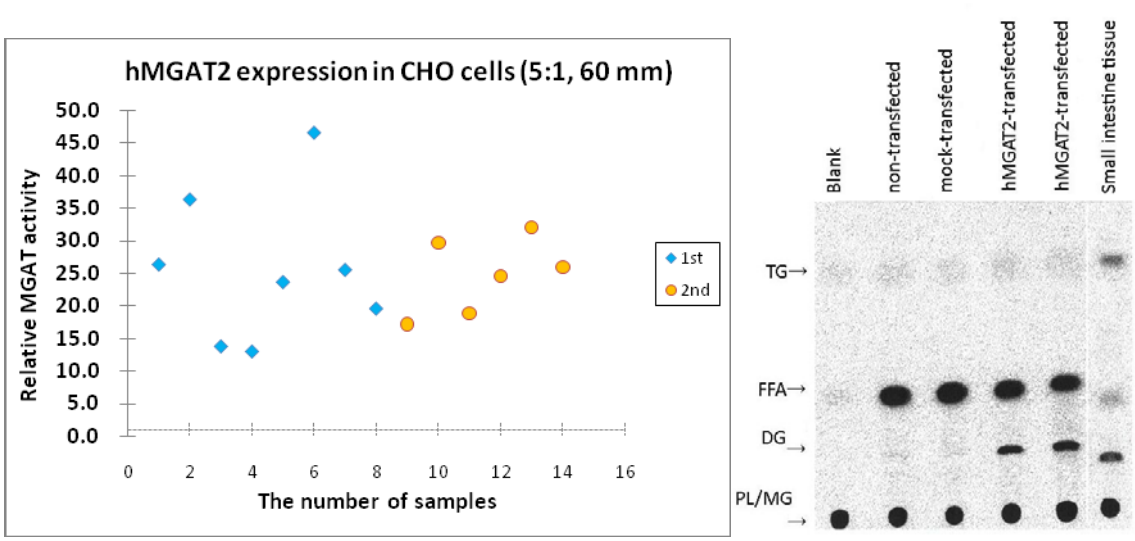

Figure 7. hMGAT2 expression in CHO-K1 cells. ***A***, The relative MGAT activity of hMGAT2 transfected CHO-K1 cells using Fugene6 (approximate reagent (µl) : DNA (µg) = 5:1) and 60 mm dishes. Each enzyme activity is calculated as described in "Materials and Methods," and results are expressed relative to empty vector-transfected controls in each separate experimental set. n = 14, total 2 sets of transfection experiments. ***B***, The representative result of the MGAT assay with samples using Fugene6 (approximate reagent (µl) : DNA (µg) = 5:1), and 60 mm dishes. For the assay, 20 µg of cell lysate protein was used.

CHO-K1 cells transfected with hMGAT2 plasmid DNA purified by PureYield Miniprep Kits in 60 mm dishes expressed noticeably higher MGAT activities than control cells transfected with empty vector (Fig 7-A). MGAT-transfected cells averaged 25.2 ± 2.4 fold higher activity than controls. There were somewhat variable relative enzyme activities, ranging from 12-fold up to 46-fold higher activity than controls.

Since all hMGAT2-transfected samples showed substantial increases of MGAT enzyme activity, we decided that FA and MG uptake and metabolism studies could be performed under this transfection condition with CHO-K1 cells, and that the results of FA and MG metabolism studies could be interpreted properly, to obtain information on the effects of MGAT on cellular lipid metabolism.

4.3. FFA uptake and metabolism in hMGAT2-transfected CHO-K1 cells

4.3.1. The net uptake of BSA-bound [^{14}C] oleic acid by hMGAT2-transfected CHO-K1 cells

The influence of MGATexpression on FFA uptake was studied using BSA-bound oleic acid with 0.02 μM of unbound FFA. Transfection was performed as described in "Materials and Methods." The hMGAT2 expressing experimental samples, and empty vector expressing control samples were incubated with radiolabeled FFA (18:1) for 2, 6, and 24 hr. Cells were collected at each time point, sonicated, and then the radioactivity in cells were determined by scintillation counting

In Fig 8, the data indicate that net uptake of BSA-bound oleic acid was continuously increased in both MGAT- and mock-transfected groups, as incubation time increased. Despite elevation of net uptake, uptake rates per hour were gradually decreased with the incubation time in both groups (data are not shown). There were no significant differences between MGAT- and mock-transfected groups at any of the time points.

Figure 8.

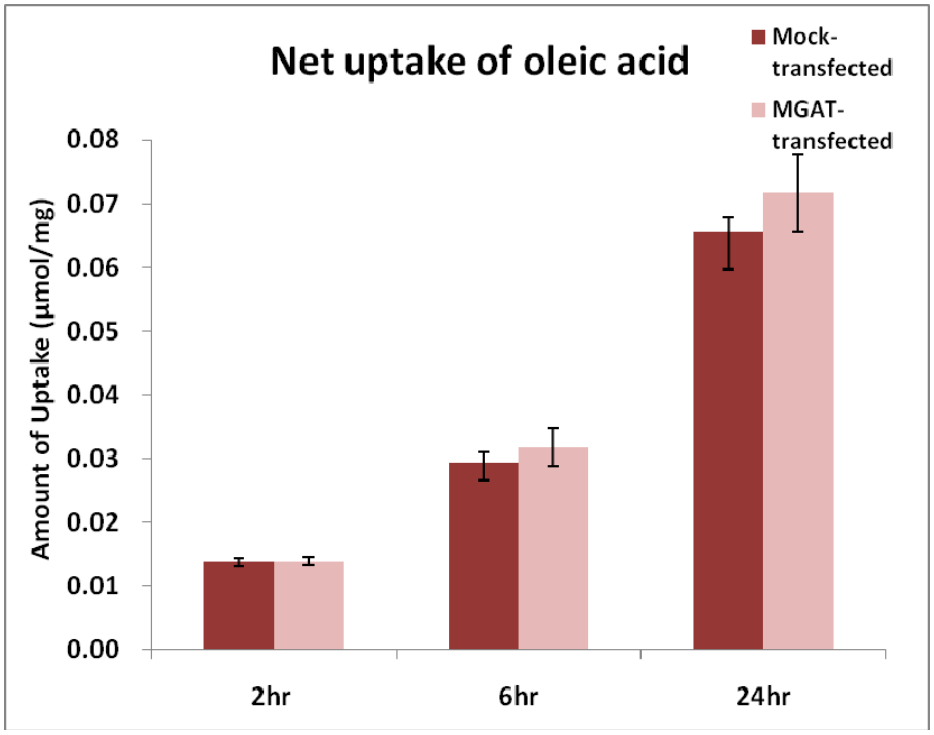

Figure 8. Net uptake of [^{14}C] oleic acid by CHO-K1 cells. Empty vector-transfected, and hMGAT2-transfected CHO-K1 cells were incubated with 30 µM of radiolabeled FFA bound to 100 µM BSA for 2, 6, and 24 hr. Harvested cells at designated time points were sonicated, and the radioactivity in cell lysates was measured as described in "Materials and Methods." Data represent the mean ± S.E.M. from n = 4 or n = 6 samples of mock-transfected cells (control) or MGAT transfected cells respectively. There were statistically no significant differences between controls and MGAT expressing cells.

Figure 9-1.

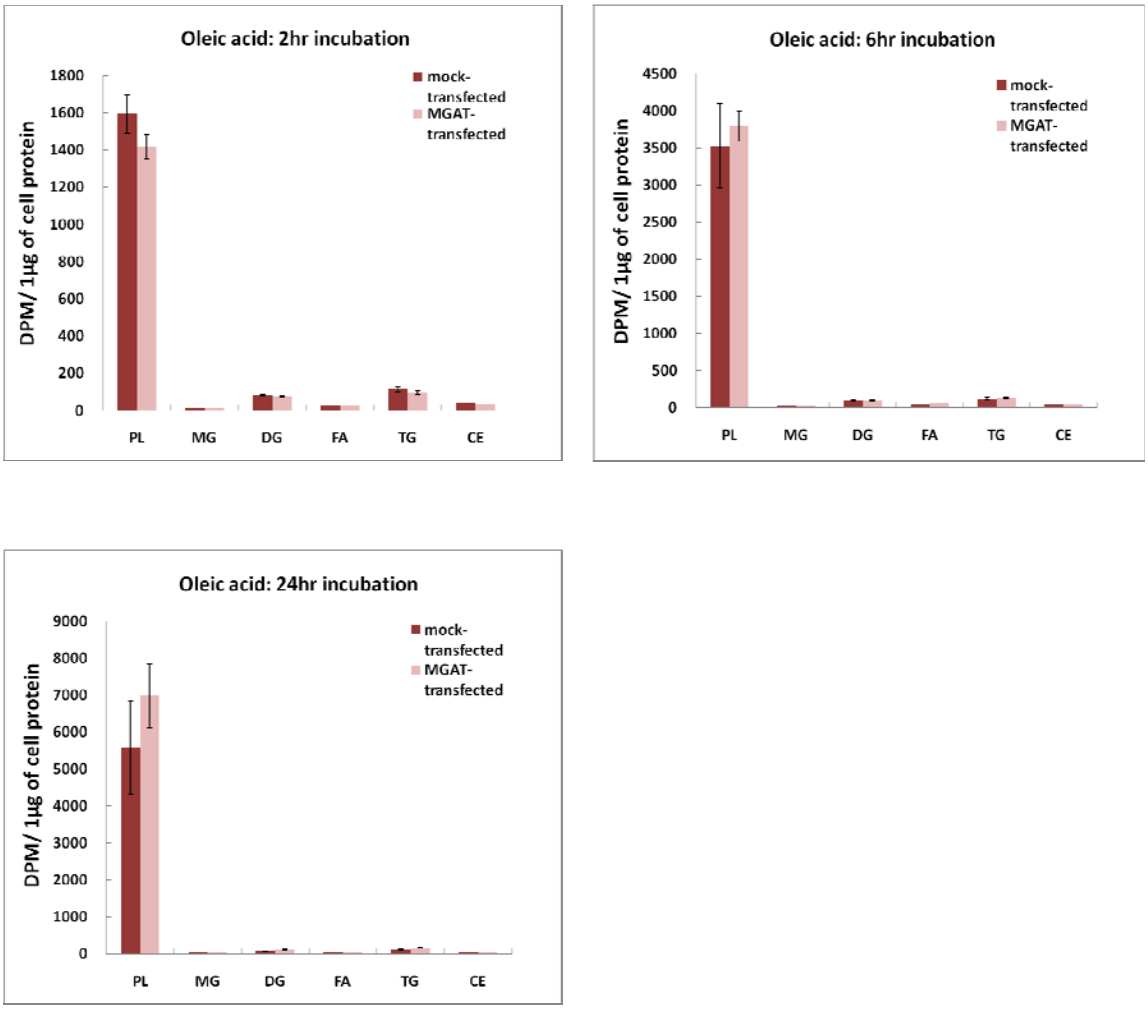

Figure 9-1. **Incorporation of [^{14}C] oleic acid into metabolites of CHO-K1 cells expressed as absolute radioactivity (DPM / 1µg of cell protein).** Empty vector-transfected, and hMGAT2-transfected CHO-K1 cells were incubated with 30 µM of radiolabeled FFA bound to 100 µM BSA for 2, 6, and 24 hr. Lipids were extracted from the harvested cells at each time point, and the cellular metabolites of radiolabeled FFA were determined by two-step TLC, as described in "Materials and Methods." Data represent the mean ± S.E.M. from n = 4 or n = 6 samples for mock-transfected cells (control) or MGAT-transfected cells, respectively. There were statistically no significant differences between controls and MGAT expressing cells.

Figure 9-2.

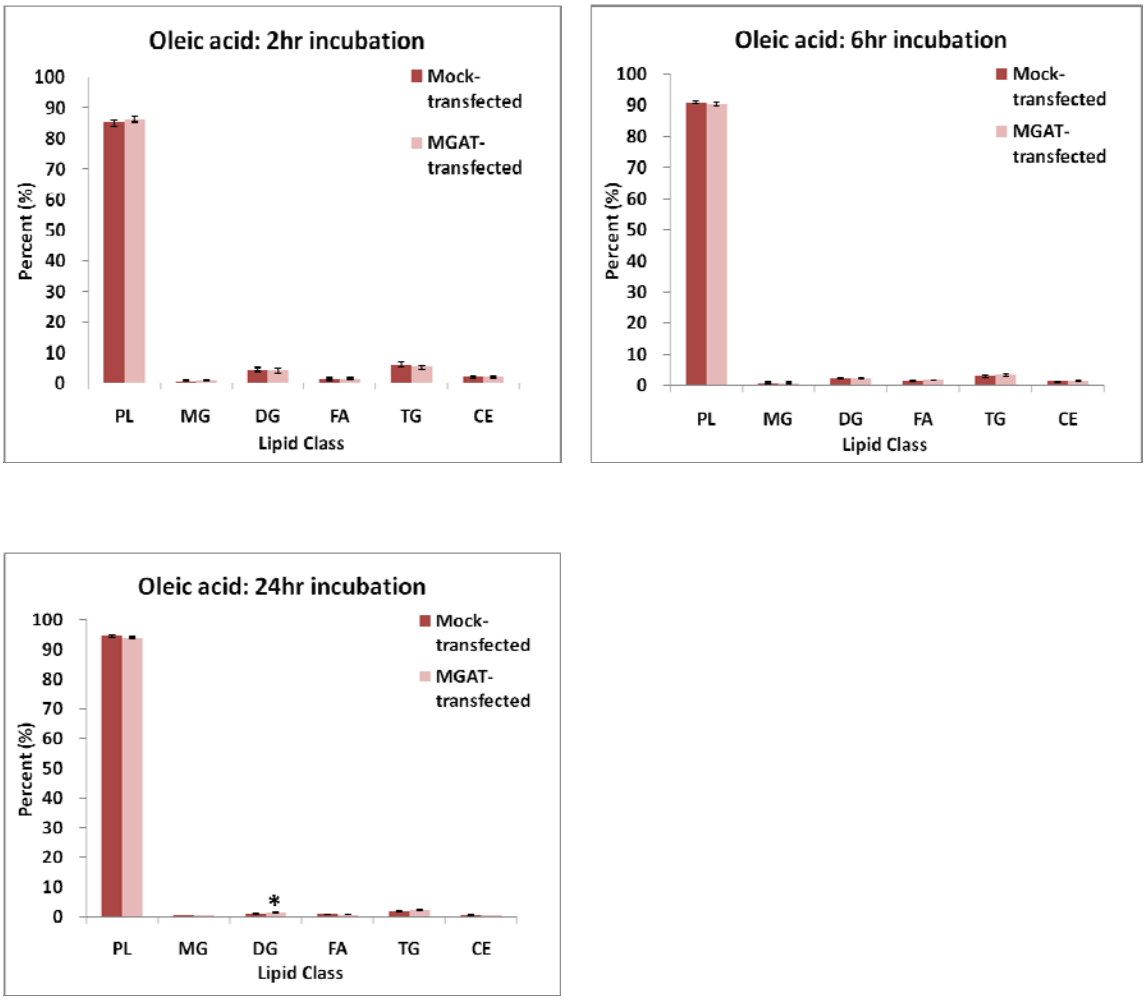

Figure 9-2. Incorporation of [^{14}C] oleic acid into metabolites of CHO-K1 cells expressed as a percentage of total incorporated lipid. Empty vector-transfected, and hMGAT2-transfected CHO-K1 cells were incubated with 30 µM of radiolabeled FFA bound to 100 µM BSA for 2, 6, and 24 hr. Lipids were extracted from the harvested cells at designated time point, and cellular metabolites of radiolabeled FFA were determined by two-step TLC, as described in "Materials and Methods." Data represent the mean ± S.E.M. from n = 4 or n = 6 samples for mock-transfected cells (control) or MGAT-transfected cells, respectively. *, $p < 0.05$ relative to control.

Table 1. Incorporation of [^{14}C] oleic acid into metabolites of CHO-K1 cells expressed as a percentage of total incorporated lipids. Data represent the mean ± S.E.M. from n = 4 or n = 6 samples for mock-transfected cells (control) or MGAT-transfected cells respectively. *, $p < 0.05$ relative to mock (control).

	Percentage of total incorporation					
	2hr		**6hr**		**24hr**	
	mock	**MGAT**	**mock**	**MGAT**	**mock**	**MGAT**
PL	85.2 ± 1.1	86.2 ± 0.9	90.9 ± 0.3	90.5 ± 0.5	94.4 ± 0.4	94.1 ± 0.3
MG	0.8 ± 0.2	1.1 ± 0.3	0.9 ± 0.3	0.8 ± 0.2	0.6 ± 0.0	0.6 ± 0.1
DG	4.5 ± 0.7	4.1 ± 0.7	2.4 ± 0.2	2.4 ± 0.1	1.2 ± 0.1	1.5 ± 0.1*****
FA	1.4 ± 0.3	1.5 ± 0.2	1.5 ± 0.2	1.7 ± 0.1	1.0 ± 0.1	0.9 ± 0.1
TG	6.1 ± 0.8	5.2 ± 0.5	3.1 ± 0.3	3.3 ± 0.3	2.0 ± 0.2	2.3 ± 0.2
CE	2.0 ± 0.2	2.0 ± 0.2	1.2 ± 0.1	1.4 ± 0.1	0.7 ± 0.1	0.8 ± 0.1

4.3.2. The incorporation of [^{14}C] oleic acid into cellular metabolites

To study the effects of MGAT expression on FFA metabolism in cells, CHO-K1 cells were transfected, as described above. A mixture of 30 μM of radiolabeled oleic acid and 100 μM BSA was used for tracking the fates of the absorbed FFA; the unbound lipid concentration was 0.02 μM. At time 0, media containing radiolabeled FFA (18:1) were added to MGAT-expressing, and empty vector-transfected (mock) cells; then samples were scraped at designated time points (2, 6, and 24 hr). Lipids were extracted from the collected cells, and the FFA metabolites were analyzed by two-step TLC, as described.

When the data were expressed as the absolute level of incorporated radioactivity into each lipid category, it was observed that the highest amount of radioactivity was found in PL in both MGAT- and mock-transfected samples (Fig 9-1). The total radioactivity incorporation into each lipid category was increased with the time of incubation in all cells. There were no statistically significant differences between the two groups.

The analyses of FFA metabolites were also evaluated as the percentage of total FFA incorporated into each of the lipid groups. The data indicated that MGAT-expressing samples and mock-transfected samples demonstrated similar results following incubation with BSA-bound FFA (18:1). Each sample incorporated most of the oleic acid into the PL fraction with 85.2 ± 1.1, 90.9 ± 0.3, and 94.4 ± 0.4 % for mock-transfected cells, and 86.2 ± 0.9, 90.5 ± 0.5, and 94.1 ± 0.3 % for MGAT-expressing cells at 2, 6, and 24 hr, respectively (Fig 9-2, Table 1). In MGAT-expressing cells, the absolute amount of DG incorporation was significantly increased at the 24 hr time point, compared to DG incorporation at 6 hr ($p < 0.05$) (Fig 9-2). This increment caused a small but significantly higher percentage of oleate incorporation into DG in MGAT-expressing cells compared to mock-transfected cells at 24 hr ($p < 0.05$) (Fig 9-2).

4.4. *sn*-2-MG uptake and metabolism in hMGAT2-transfected CHO-K1 cells

4.4.1. The net uptake of BSA-bound [^{3}H] *sn*-2-monoolein by hMGAT2-transfected CHO-K1 cells

The influence of MGAT expression on net MG uptake was determined. MGAT expressing or empty vector (mock) transfected cells were incubated with 30 μM of BSA-bound *sn*-2-monoolein for designated times (2, 6, and 24 hr). Cells were collected at each time point, sonicated, and total radioactivity in cell lysates was measured.

In contrast with the net uptake of FFA, the uptake of MG showed significant differences between mock- and MGAT-expressing cells. Compared to the net uptake of MG in mock-transfected cells with 0.005 ± 0.001, 0.003 ± 0.001, and 0.002 ± 0.001 μmol/ mg at 2, 6, and 24 hr respectively, MGAT-transfected cells took up significantly higher amounts of MG from the initial time point to the end point with 0.008 ± 0.001, 0.006 ± 0.001, and 0.003 ± 0.001 μmol/mg at 2, 6, and 24 hr respectively (Fig 10).

We observed that the total incorporation of MG (18:1) into cells decreased as incubation time increased in both MGAT- and mock-transfected cells (Fig 10). In order to try and determine where the reduced radioactivity went, we measured the changes of radioactivity in the media, because we expected that if the radiolabeled MG was taken up and oxidized incompletely, radioactivity might be increased in the media from water soluble intermediate oxidation products.

As shown in Fig 11-A, in MGAT samples and mock samples, radioactivity in the media was decreased at 2 hr and 6 hr. The radioactivity in the media of the MGAT samples was lower than in the mock samples at all time points, which indicates that MGAT expressing cells absorbed more MG; this is consistent with the results of the net uptake study. The calibrated radioactivity in media and cells of both groups was normalized by control radioactivity (no cells) at corresponding time points. The expected radioactivity for cells was calculated by subtraction of

Figure 10.

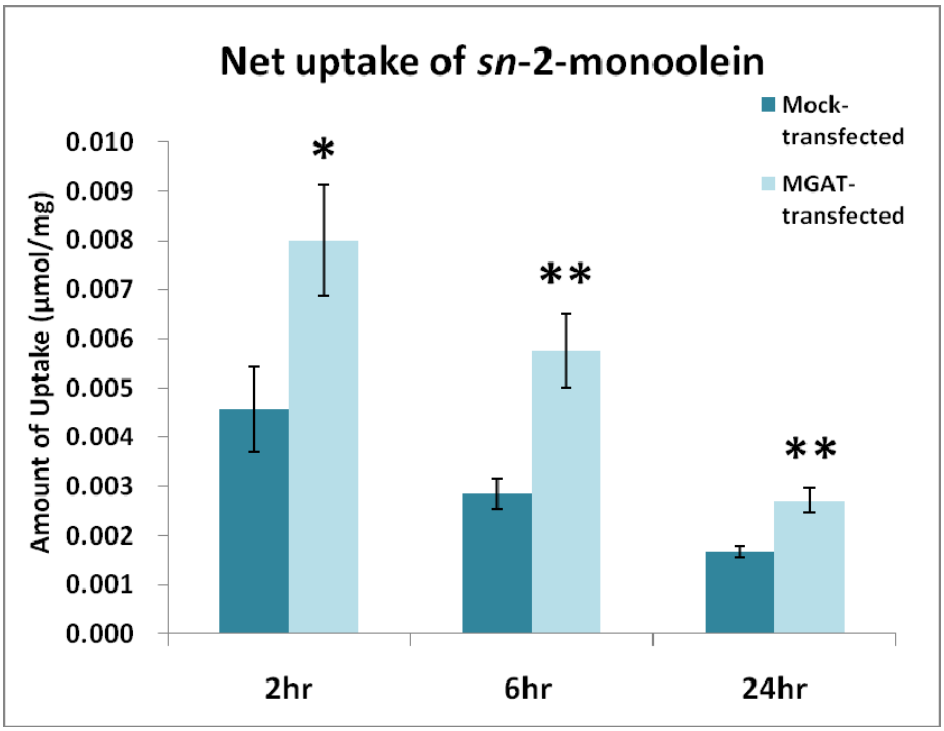

Figure 10. Net uptake of [^{3}H] *sn*-2- monoolein by CHO-K1 cells. Empty vector-transfected, and hMGAT2-transfected CHO-K1 cells were incubated with 30 µM of radiolabeled MG bound to 100 µM BSA for 2, 6, and 24 hr. Harvested cells at designated time points were sonicated, and the radioactivity in cell lysates was measured as described in "Materials and Methods." Data represent the mean ± S.E.M. from n = 5 or n = 5~ 6 samples of mock-transfected cells (control) or MGAT-transfected cells respectively. *, $p < 0.05$; **, $p < 0.01$ relative to control.

Figure 11

A.

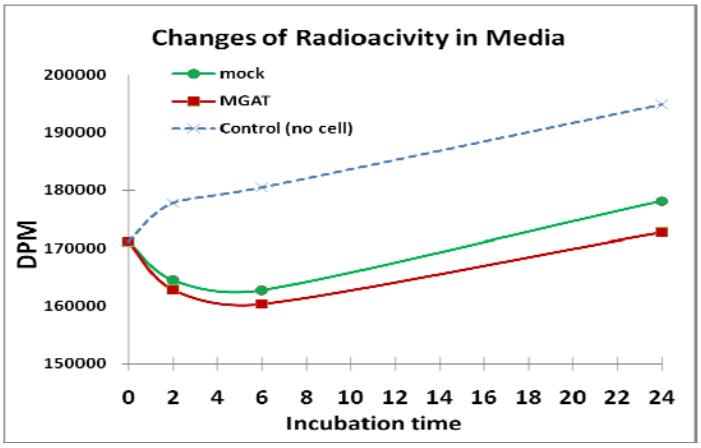

B.

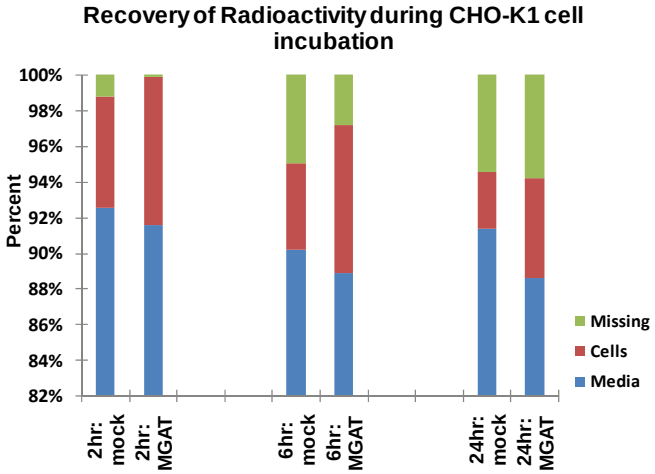

Figure 11. Radioactivity changes during incubation with [^{3}H] *sn*-2-monoolein in CHO-K1 cells. ***A.*** Radioactivity changes in media containing 30 µM of radiolabeled MG bounded to 100 µM BSA were observed for each designated time point. n = 2 ***B.*** Radioactivity changes in media and cells were measured during the incubation with 30 µM of radiolabeled MG bound to 100 µM BSA for 2, 6, and 24 hr. Missing DPM was calculated by subtraction of DPM in culture media and cell homogenates from control DPM (no cell) in media at the corresponding time points. Data are expressed as the percentage of total DPM. n = 2

sample radioactivity in media from control radioactivity in media at each time point. Then, the expected radioactivity found in cells was compared with actual radioactivity measurements of the cell lysates, and by the subtraction of the actual radioactivity in cell lysates from the expected radioactivity found in cells, the missing radioactivity was calculated (Fig 11-B). The results indicate that with increasing incubation time, the percentage of missing radioactivity was increased; this was consistent with the reduced net uptake of MG with incubation time. Based on these results, we suggest that cells metabolize the radiolabeled MG into CO_2 gas; thus, the reduction of MG net uptake could be due to β-oxidation. At 2 hr and 6 hr time points, the MGAT-expressing cells had lower levels of missing radioactivity / CO_2 , but at 24 hr MGAT and mock-transfected cells were equivalent. As indicated in Fig 11-A, and Fig 11-B, MGAT-expressing cells absorbed higher levels of radiolabeled MG from media; furthermore, we hypothesize that oxidation was less vigorous than empty vector-transfected (mock) cells. To summarize, MGAT-expressing cells showed statistically significantly higher net uptake of MG compared to empty vector-transfected mock cells.

4.4.2. The incorporation of [^{3}H] *sn*-2-monoolein into cellular metabolites

The influence of MGAT expression on cellular utilization of absorbed MG was studied. The hMGAT2-transfected and empty vector-transfected CHO-K1 cells were incubated with 30 μM of radiolabeled *sn*-2-monoolein bound to 100 μM of BSA for 2, 6, and 24 hr. The unbound lipid concentration of BSA-bound MG was 0.09 μM. Lipids were extracted from the harvested cells at each time point, as described under "Materials and Methods," and the incorporation of MG into each lipid group was analyzed by two-step TLC, and scintillation counting of individual spots.

When cells were incubated with MG (18:1), the absolute amounts of radioactivity incorporated into TG, as well as DG, were significantly increased in MGAT-expressing cells (Fig 12-1). Generally, MGAT-expressing cells showed higher radioactivity in all lipid categories at all time points, compared to the mock-transfected cells, and the increases in PL, DG, and TG incorporation were statistically significant.

As shown in Fig 12-2, when the data were described as a percentage of the total radioactivity incorporation, both MGAT-expressing samples and mock-expressing samples showed the highest incorporation into the PL fraction; however, in contrast with FFA metabolites, both groups also showed a high level of incorporation of labeled MG into TG. Moreover, the metabolic fate of MG in hMGAT2 expressing cells was remarkably different from that of empty vector-transfected cells. At the 2 hr time point, as mentioned above, MGAT-expressing cells incorporated approximately 2-fold higher level of radioactivity into DG (8.8 ± 1.5 %) than empty vector expressed cells (4.7 ± 0.7 %). At all time points, MGAT-transfected cells had significantly higher percent PL incorporation with 53.4 ± 3.1, 66.6 ± 2.5, and 77.5 ± 1.9 %, and lower TG incorporation with 31.1 ± 0.8, 24.5 ± 1.5, and 14.2 ± 1.0 % compared to mock-transfected cells (Fig 12-2, Table 2-A). Thus, the TG:PL ratios were generally lower in MGAT-expressing cells than those of mock-transfected cells, and at the 6 hr and 24 hr time points, differences were statistically significant ($p < 0.01$) (Table 2-B). This suggests that in CHO-K1 cells, *sn*-2-monoolein is preferentially used to synthesize PL rather than TG, and that increased expression of hMGAT2 resulted in a further partitioning of MG into PL relative to TG.

Figure 12-1.

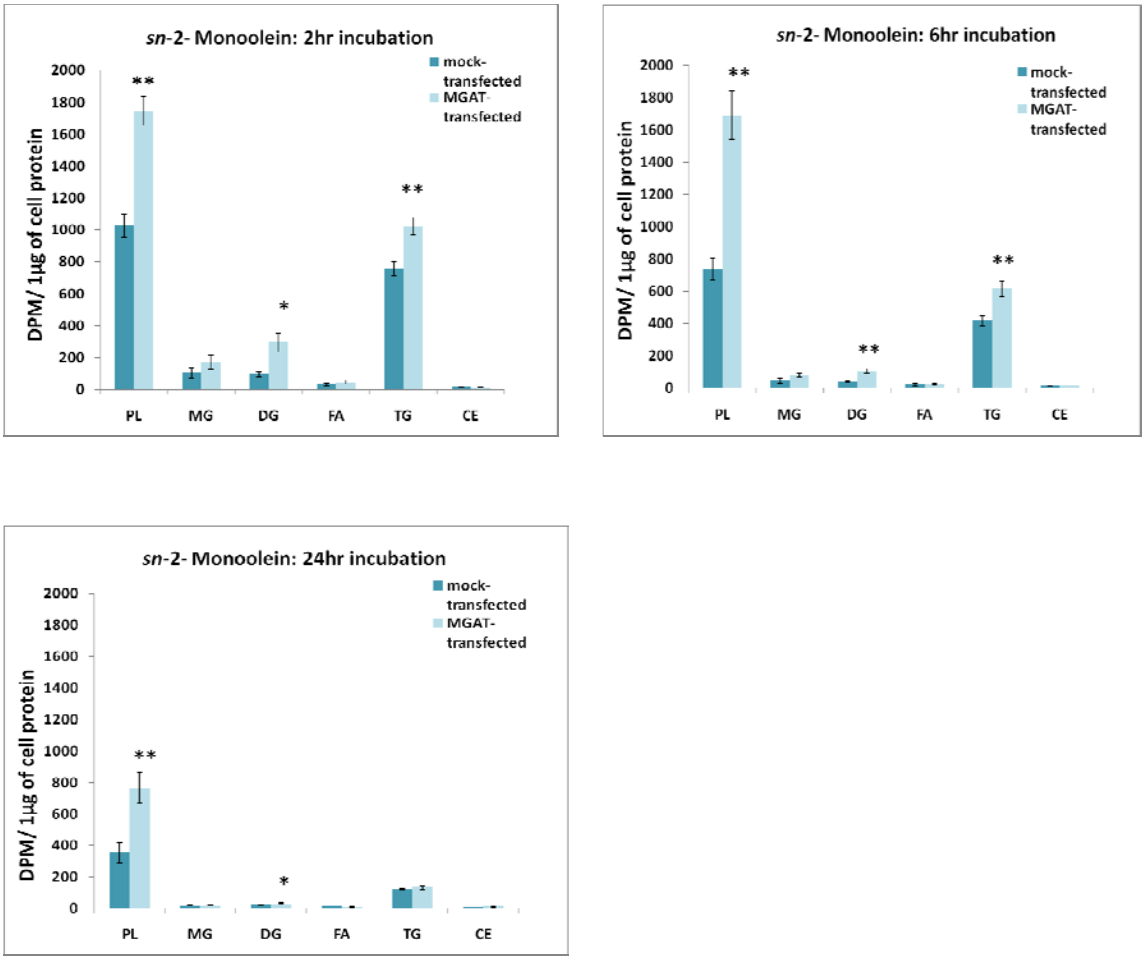

Figure 12-1. Incorporation of [^{3}H] *sn*-2 monoolein into metabolites of CHO-K1 cells expressed as absolute radioactivity (DPM / 1µg of cell protein). Empty vector-transfected, and hMGAT2 -transfected CHO-K1 cells were incubated with 30 µM of radiolabeled MG bound to 100 µM BSA for 2, 6, and 24 hr. Lipids were extracted from the harvested cells at each time point, and the cellular metabolites of radiolabeled MG were determined by two-step TLC as described in "Materials and Methods." Data represent the mean ± S.E.M. from n = 5 or n = 6 samples for mock-transfected cells (control) or MGAT-transfected cells, respectively. *, $p < 0.05$; **, $p < 0.01$ relative to control.

Figure 12-2.

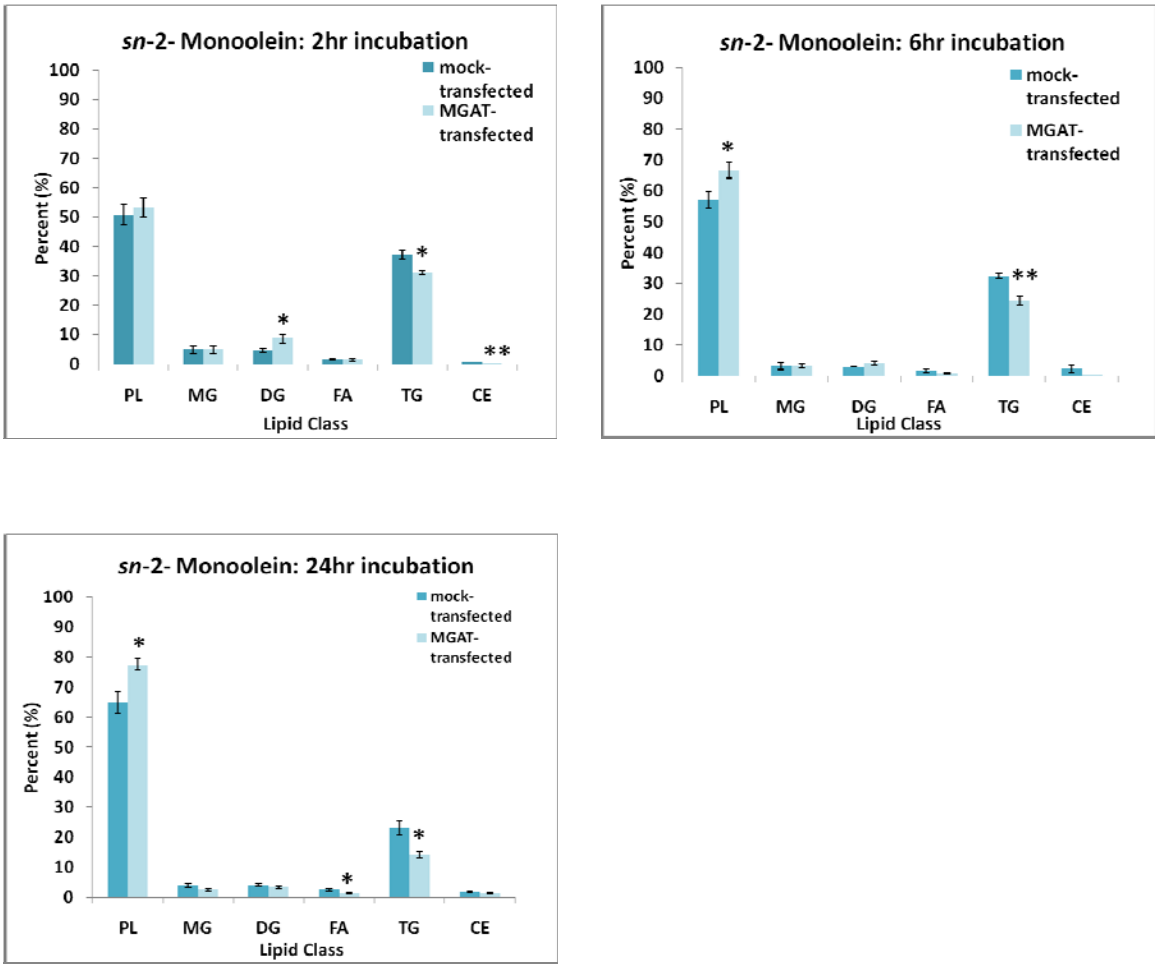

Figure 12-2. Incorporation of [^{3}H] *sn*-2-monoolein into metabolites of CHO-K1 cells expressed as a percentage of total incorporated lipids. Empty vector-transfected, and hMGAT2-transfected CHO-K1 cells were incubated with 30 µM of radiolabeled MG bounded to 100 µM BSA for 2, 6, and 24 hr. Lipids were extracted from the harvested cells at designated time points, and cellular metabolites of radiolabeled MG were determined by two-step TLC as described in "Materials and Methods." Data represent the mean ± S.E.M. from n = 5 or n = 6 samples for mock transfected cells (control) or MGAT transfected cells, respectively. *, $p < 0.05$; **, $p < 0.01$ relative to control.

Table 2-A. Incorporation of [^{3}H] *sn*-2-monoolein into metabolites of CHO-K1 cells expressed as a percentage of total incorporated lipid. Data represent the mean ± S.E.M. from n = 5 or n = 6 samples for mock-transfected cells (control) or MGAT-transfected cells respectively. *, $p < 0.05$; **, $p < 0.01$ relative to mock (control).

	Percentage of total incorporation					
	2hr		**6hr**		**24hr**	
	mock	**MGAT**	**mock**	**MGAT**	**Mock**	**MGAT**
PL	50.9 ± 3.6	53.4 ± 3.1	57.1 ± 2.5	66.6 ± 1.3*****	64.8 ± 3.6	77.5 ± 0.2*****
MG	5.0 ± 1.3	5.0 ± 1.2	3.3 ± 1.2	3.2 ± 0.6	3.8 ± 0.6	2.4 ± 0.5
DG	4.7 ± 0.7	8.8 ± 1.5*****	3.0 ± 0.1	4.1 ± 0.5	4.1 ± 0.4	3.4 ± 0.4
FA	1.5 ± 0.3	1.4 ± 0.4	1.8 ± 0.6	1.0 ± 0.2	2.4 ± 0.3	1.2 ± 0.2*****
TG	37.3 ± 1.5	31.1 ± 0.8*****	32.4 ± 0.7	24.5 ± 1.5******	23.1 ± 2.2	14.2 ± 1.0*****
CE	0.7 ± 0.1	0.4 ± 0.1******	2.4 ± 1.3	0.6 ± 0.1	1.7 ± 0.2	1.2 ± 0.2

Table 2-B. TG : PL ratio for [^{3}H] *sn*-2-monoolein by CHO-K1 cells.

	2hr	**6hr**	**24hr**
mock	0.8 ± 0.1	0.6 ± 0.1	0.4 ± 0.1
MGAT	0.6 ± 0.1	0.4 ± 0.1******	0.2 ± 0.1******

Chapter V. Discussion

FFA and *sn*-2-MG are the major digestive products of dietary TG in the small intestinal lumen, and following their absorption, they are reconstituted to TG in the enterocyte mainly by the MGAT pathway. Despite the important role of MGAT in dietary lipid assimilation in the small intestine, the detailed mechanisms are not completely understood. To explore the influence of MGAT expression on FFA and *sn*-2-MG uptake and metabolism in the enterocyte, the Caco-2 human colorectal cancer cell line was selected as the most relevant cell model. However because of inconsistent MGAT expression in Caco-2 cells, the CHO-K1 cell line which is known for easier introduction of foreign DNA and has little basal MGAT activity, was ultimately used for these studies. The MGAT-transfected CHO-K1 cells demonstrated consistent MGAT expression, and averaged approximately 25-fold higher enzyme activity than empty vector-transfected controls.

The main results of these studies are as follows (discussion and speculation will follow):

1) Net uptake of MG, but not FFA, was greater in MGAT-transfected cells.

2) A decrement in *sn*-2-MG net uptake as a function of time in CHO cells was likely caused by the β-oxidation of the absorbed lipid.

3) The uptake ratio of FFA to MG in CHO cells was approximately 2 : 1, which fits the stoichiometric ratio to resynthesize TG, which is generated from 2FA and a single MG.

4) Metabolism of MG, but not FFA, was altered in MGAT-transfected cells. Specifically, incorporation of MG into DG and TG were increased compared to mock-transfected cells

5) MG is mostly channeled into PL in CHO cells.

In the current experiment, cells cultured with *sn*-2-MG demonstrated remarkable differences between mock-transfected and MGAT-expressing cells: MGAT-expressing cells absorbed significantly higher amounts of *sn*-2-MG during all the designated time points compared to mock-transfected cells. When the mock-transfected and MGAT-expressing cells were incubated with FFA for the designated time points, the net uptake of FFA in both groups showed no significant difference. In addition, MGAT expressing cells incubated with FFA incorporated similar amounts of radioactivity into each lipid class as did the mock expressing cells, but MGAT expressing cells incubated with MG for 24h accumulated slightly greater amounts of radioactivity in DG, which is known to be catalyzed by the MGAT enzyme. It is not clear that this small increase, though statistically significant, is biologically important.

We speculate that the activity of MGAT enzyme is related with the presence of MG adjacent to the plasma membrane. Yen and Farese demonstrated that hMGAT2 had a much higher K_m for MG (~ 45 μM) than the concentration of MG normally found in the cell membrane, and based on this finding they concluded that the activity of MGAT is dependent on the MG concentration (77). However, it must also be considered that in the present experiment, the enzyme activity in the MGAT expressing cells was less than 10 % of MGAT activity in an intact rat jejunum (72,104,105); therefore, there is a possibility that the absence of a significant difference in FFA uptake between both groups was caused by relatively low enzyme activity in MGAT expressing cells. Nevertheless the significant changes in MG uptake and metabolism suggest that MGAT expression altered MG disposition specifically.

We expected that the net uptake of MG in CHO cells would increase during the incubation, similar to what we observed for the net uptake of FFA or the net uptake of MG in Caco-2 cells (96), but the total uptake of MG in CHO cells decreased as a function of incubation time. To determine where the decreased radiolabeled MG went, we measured three compartments: 1) the radioactivity in cell culture media 2) the radioactivity in cell lysates 3) the

radioactivity in media without cells, as a control. As the radioactivity in the cell culture media was compared to the radioactivity in control (no cells), we observed that the radioactivity in cell culture media was gradually decreased and below the control at all time points, which indicates that the cells absorbed radiolabeled MG continuously. However, when the radioactivity in media was added up with the radioactivity found in cell homogenates, we found out that some of the radioactivity had "disappeared." This missing radioactivity was increased as the incubation time increased, which is consistent with the observed reduction of net uptake in cells. We speculate that if the MG with the radioactive label on its glycerol backbone was oxidized incompletely, radioactivity might be found in the media as water soluble intermediates. However, as mentioned above, the radioactivity in the cell culture media was gradually reduced. This suggests that CHO cells absorbed the MG and turned it into an undetectable form, such as CO_2, which means, i.e., the β-oxidation of lipid leads to the reduction of total incorporation of MG into CHO cells during the incubation. We also suggest that MGL, which is known to catalyze the hydrolysis of *sn*-2-MG, and has detectable mRNA expression in various tissues including ovary (95), could be involved in the complete oxidation of MG by hydrolyzing it to FA and glycerol. However, it should be noted that MGL is actually expressed in CHO-K1 cells. CHO cells are ovarian fibroblasts, which are not differentiated, so that they do not express the functional characteristics found in the mature ovary.

The net uptake of MG in MGAT-expressing cells was significantly higher than in mock expressing cells at all time points, which is consistent with the lower radioactivity in MGAT expressing cell culture media compared to radioactivity in media of mock-transfected cells. Moreover, the higher incorporation of MG in MGAT-expressing cells is inversely related to the "disappeared" radioactivity in cells, which was less than that of mock cells. Chon ***et al.*** showed that over-expression of intestinal MGL down-regulates the MGAT2 gene expression in the enterocyte (106). It is therefore possible that in this study the attenuation of lipid oxidation in the

MGAT expressing cells was caused by the down-regulated endogenous MGL expression due to the ectopic expression of MGAT enzyme. Since the mock-transfected cells only have the G-3-P pathway, this observation indicates that the expression of MGAT influences the uptake of MG into cells via the MGAT pathway, which is more effective to esterify absorbed *sn*-2-MG into TG or PL than the G-3-P pathway, and maintains the concentration gradient of MG across the plasma membrane, allowing continuous uptake into cells (2). Additionally, it has been suggested that the saturable function of MG uptake at a low monomer concentration ($\leq$ 6.5 μM) indicates a protein-mediated transport mechanism in the enterocyte (55). Although the CHO cell line is not an ideal model to study lipid uptake by the enterocyte, MGAT-expressing cells showed significantly increased MG uptake at a 0.09 μM monomer concentration, suggesting that the transmembrane proteins, which are thought to play an important role in lipid uptake (56), may be influenced by MGAT expression in cells.

The net uptake ratio of FFA to MG in CHO-K1 cells was evaluated at each time point. Since the total uptake of MG into cells decreased as a function of incubation time, it was hard to compare the net uptake of FFA to MG, but at the initial time point, mock-transfected and MGAT-expressing CHO cells demonstrated a 2.8 : 1 or 1.75 : 1 ratio of FFA to MG uptake, respectively. Interestingly, this is consistent with a previous uptake study at the apical surface of Caco-2 cells (54), which showed that the ratio of the average V_{max} of FFA to that of MG was approximately 2 : 1. This also fits the stoichiometric ratio of FFA to MG to reconstitute TG in the enterocyte. In the previous study, it was suggested that high expression of L-FABP in Caco-2 cells, which has a stronger binding affinity for oleate compared to monoolein, may play an important role for the higher uptake capacity of Caco-2 cells for FFA (54). It is known that two FABPs, heart-FABP (H-FABP) and Ileal FABP (I-LBP), are highly expressed in ovary tissue (107,63). As mentioned previously, CHO cells are fibroblasts, which are not differentiated into functional ovary cells, therefore, the expression of FABP in CHO-K1 cells should be experimentally determined. Both

H-FABP and I-LBP are high affinity binders for FFA, especially oleate; therefore similar to Caco-2 cells, it is possible that H-FABP and I-LBP may influence the higher uptake capacity of CHO-cells for FFA.

The metabolic fate of MG in MGAT-expressing cells is significantly different from that in mock-transfected cells, in which lipid synthesis proceeds mainly via the G-3-P pathway. In mammals, there are two major biochemical pathways to synthesize TG: G-3-P and MGAT pathways. Since in most tissues, the synthesis of TG is primarily by the G-3-P pathway, we considered that the mock-transfected CHO cells metabolized the absorbed lipids via this pathway. On the other hand, the MGAT pathway is predominant in the hepatocyte, enterocyte, and adipocyte where significant amounts of TG is synthesized and stored (108), so that we transiently transfected CHO cells, which have an undetectable level of MGAT expression, with hMGAT2. Thus MGAT-transfected cells could metabolize at least some of the absorbed FFA and MG via the MGAT pathway. As shown in Fig 1-4, the G-3-P and MGAT pathways share the common metabolic intermediate, *sn*-1,2-DG, which is precursor of both TG and certain PL such as PC. It has been questioned whether each pathway is merged into the same pool of DG or whether there are separate DG pools (69).

In the current study, when mock and MGAT expressing cells were incubated with radiolabeled MG, MGAT expressing cells incorporated higher level of radioactivity into each lipid class compared to mock expressing cells, which is consistent with the net uptake study; the increased incorporation into DG and TG, as well as PL was statistically significant. In addition, when the cellular metabolites in MGAT expressing cells was evaluated by the percentage of total MG incorporation into each lipid class, we could observe the tendency of MGAT-expressing cells to show significantly higher percent PL incorporation and lower percent TG incorporation relative to mock-transfected cells, and this was intensified as a function of incubation time. This

difference in metabolic partitioning of MG in mock and MGAT expressing cells indicates that DG synthesized from the G-3-P and MGAT pathways may not be equivalent.

Compared with a previous study, in which Caco-2 cells incorporated lipids from the apical surface primarily into TG (32), in this study CHO-K1, which has limited capacity for lipid storage, incorporated absorbed lipids primarily into PL. Initially we expected a higher percent incorporation of MG into TG in MGAT-expressing cells compared to mock expressing cells, because it has been suggested that DG synthesized from MGAT is directed to TG synthesis only (109,69). However, as described above, MGAT-expressing cells incorporated a greater percent of MG into PL rather than TG, and this may indirectly indicate that MGAT expression influenced CTP: phosphocholine cytidyltransferase, which is the rate limiting step to synthesize PC, and regulates DG flux (110)

This study has a limitation, which is that the CHO-K1 cell line is not an ideal model to explore the cellular lipid metabolism of the human enterocyte. Therefore for future studies, it is necessary to improve transfection methods for the Caco-2 cell line, which is the most relevant cell model, but also known to be a difficult cell line in which to introduce foreign DNA. Moreover, for the better understanding of lipid uptake into cells, it is necessary to measure the expression of transmembrane lipid transport proteins such as FABPpm and FATP, and intracellular FABP levels, especially H-FABP and I-LBP, in CHO-K1 cells. It will also be interesting to explore if there are any changes in PC biosynthesis enzymes by MGAT expression in CHO cells.

References

1. The Gut: Inner Tube of Life [Internet]. [cited 2010 Feb 20];Available from: http://www.sciencemag.org/sciext/gutposter/

2. Tso P, Crissinger K. Digestion and absorption of lipids. In: Biochemical and Physiological Aspects of Human Nutrition. W.B. Saunders Company; 2000. p. 125-141.

3. Carey MC, Small DM, Bliss CM. Lipid Digestion and Absorption. Annu. Rev. Physiol. 1983 3;45(1):651-677.

4. Cases S, Stone SJ, Zhou P, Yen CE. Cloning of DGAT2, a Second Mammalian Diacylglycerol Acyltransferase, and Related Family Members. J. Biol. Chem. 2001 Jul 31;276:38870-38876.

5. Gray H. The Digestive Apparatus: the small intestine. In: Anatomy of the Human Body. Philadelphia: Lea & Febiger; 1985.

6. Schofield G. Anatomy of muscular and neural tissues in the alimentary canal. In: Code C, editor. Handbook of physiology, Section 6, Vol 4: Motility. Baltimore: Williams & Wilkins; 1968. p. 1579-1627.

7. Stanfield CL, Germann WJ. The gastrointestinal system. In: Principles of Human Physiology (3rd Edition). Benjamin Cummings; 2007. p. 569-604.

8. Radtke F, Clevers H. Self-Renewal and Cancer of the Gut: Two Sides of a Coin. Science. 2005 Mar 25;307(5717):1904-1909.

9. Tso P, Crissinger K. Overview of digestion and absorption. In: Biochemical and Physiological Aspects of Human Nutrition. W.B. Saunders Company; 2000. p. 75-90.

10. Weisbrodt N. Motiity of the small intestine. In: Physiology of the Gastrointestinal Tract, Volume 1. New York: Raven Press; 1987.

11. Chen M, Yang Y, Braunstein E, Georgeson KE, Harmon CM. Gut expression and regulation of FAT/CD36: possible role in fatty acid transport in rat enterocytes. Am J Physiol Endocrinol Metab. 2001 Nov 1;281(5):E916-923.

12. Storch, J., Herr, F.M. Nutritional regulation of fatty acid transport protein expression. In: Nutrient-Gene Interactions in Health and Disease. CRC Press; 2001.

13. Cao J, Hawkins E, Brozinick J, Liu X, Zhang H, Burn P, et al. A predominant role of acyl-CoA:monoacylglycerol acyltransferase-2 in dietary fat absorption implicated by tissue distribution, subcellular localization, and up-regulation by high fat diet. J. Biol. Chem. 2004 Apr 30;279(18):18878-18886.

14. Buhman KK, Smith SJ, Stone SJ, Repa JJ, Wong JS, Knapp FF, et al. DGAT1 is not essential for intestinal triacylglycerol absorption or chylomicron synthesis. J. Biol. Chem. 2002 Jul 12;277(28):25474-25479.

15. Hall PA, Coates PJ, Ansari B, Hopwood D. Regulation of cell number in the mammalian gastrointestinal tract: the importance of apoptosis. J. Cell. Sci. 1994 Dec;107 (Pt 12):3569-3577.

16. Madara, J.L., Trier, J.S. Functional morphology of the mucosa of the small intestine. In: Physiology of the Gastrointestinal Tract, Volume 2. New York: Raven Press; 1987. p. 1209-1249.

17. Sukhotnik I, Coran AG, Mogilner JG, Shamian B, Karry R, Lieber M, et al. Leptin Affects Intestinal Epithelial Cell Turnover in Correlation With Leptin Receptor Expression Along the Villus-Crypt Axis After Massive Small Bowel Resection in a Rat. Pediatric Research. 2009 12;66(6):648-653.

18. Shiner, M. Ultrastructure of the small intestinal mucosa. New York: Spriner-Verlag Berlin Heigelgerg; 1983. p. 61-78.

19. Shiau YF, Boyle JT, Umstetter C, Koldovsky O. Apical distribution of fatty acid esterification capacity along the villus-crypt unit of rat jejunum. Gastroenterology. 1980 Jul;79(1):47-53.

20. O'Doherty PJA. Phospholipid synthesis in differentiating cells of rat intestine. Archives of Biochemistry and Biophysics. 1978 Oct;190(2):508-513.

21. Fish EM, Molitoris BA. 0.Alterations in Epithelial Polarity and the Pathogenesis of Disease States. N Engl J Med. 1994 Jun 2;330(22):1580-1588.

22. Barbieri D, de Brito T, Hoshino S, Nascimento F OB, Campos JVM, Quarentei G, et al. Giardiasis in Childhood. Arch Dis Child. 1970 Aug;45(242):466-472.

23. Histological demonstration of mucosal invasion by Giardia lamblia in man. Gastroenterology. 1967 Feb 1;52(2):143.

24. Groff JL. The digestive system: Mechanism for nourishing the body. In: Advanced Nutrition and Human Metabolism. Belmont, CA: West/Wadsworth, 1999; p. 24-52.

25. Ito S. Structure and function of the glycocalyx. Fed. Proc. 1969 Feb;28(1):12-25.

26. Quaroni A, Kirsch K, Weiser MM. Synthesis of membrane glycoproteins in rat small-intestinal villus cells. Effect of colchicine on the redistribution of L-[1,5,6-3H]fucose-labelled membrane glycoproteins among Golgi, lateral basal and microvillus membranes. Biochem. J. 1979 Jul 15;182(1):213-221.

27. Weiser MM, Neumeier MM, Quaroni A, Kirsch K. Synthesis of plasmalemmal glycoproteins in intestinal epithelial cells. Separation of Golgi membranes from villus and crypt cell surface membranes; glycosyltransferase activity of surface membrane. J. Cell Biol. 1978 Jun;77(3):722-734.

28. Schaffer JE, Lodish HF. Expression cloning and characterization of a novel adipocyte long chain fatty acid transport protein. Cell. 1994 Nov 4;79(3):427-436.

29. Gangl A, Ockner RK. Intestinal metabolism of plasma free fatty acids. Intracellular

compartmentation and mechanisms of control. J. Clin. Invest. 1975 Apr;55(4):803-813.

30. Gangl A, Renner F. In vivo metabolism of plasma free fatty acids by intestinal mucosa of man. Gastroenterology. 1978 May;74(5 Pt 1):847-850.

31. Trotter PJ, Storch J. Fatty acid uptake and metabolism in a human intestinal cell line (Caco-2): comparison of apical and basolateral incubation. J. Lipid Res. 1991 Feb;32(2):293-304.

32. Ho S, Delgado L, Storch J. Monoacylglycerol Metabolism in Human Intestinal Caco-2 Cells. EVIDENCE FOR METABOLIC COMPARTMENTATION AND HYDROLYSIS. J. Biol. Chem. 2002 Jan 11;277(3):1816-1823.

33. Storch J, Zhou YX, Lagakos WS. Metabolism of apical versus basolateral sn-2-monoacylglycerol and fatty acids in rodent small intestine. J. Lipid Res. 2008 Aug;49(8):1762-1769.

34. Patton, J.S. Gastrointestinal lipid digestion. In: Physiology of the Gastrointestinal Tract. New York: Raven Press; 1981. p. 1123-1146.

35. Hui DY, Howles PN. Carboxyl ester lipase: structure-function relationship and physiological role in lipoprotein metabolism and atherosclerosis. J. Lipid Res. 2002 Dec 1;43(12):2017-2030.

36. Duan, R. Enzymatic aspects of fat digestion in the gastrointestinal tract. In: Fat digestion and absorption. The American Oil Chemists Society; 2000. p. 25-46.

37. Groff JL. Lipds. In: Advanced Nutrition and Human Metabolism. Belmont, CA: West/Wadsworth, 1999; p. 123-162.

38. Lowe ME. Properties and function of pancreatic lipase related protein 2. Biochimie. 2000 Nov;82(11):997-1004.

39. Lowe ME, Kaplan MH, Jackson-Grusby L, D'Agostino D, Grusby MJ. Decreased Neonatal Dietary Fat Absorption and T Cell Cytotoxicity in Pancreatic Lipase-related Protein 2-Deficient Mice. Journal of Biological Chemistry. 1998 Nov 20;273(47):31215-31221.

40. Hui DY, Howles PN. Carboxyl ester lipase: structure-function relationship and physiological role in lipoprotein metabolism and atherosclerosis. J. Lipid Res. 2002 Dec 1;43(12):2017-2030.

41. Wang CS, Kuksis A, Manganaro F, Myher JJ, Downs D, Bass HB. Studies on the substrate specificity of purified human milk bile salt-activated lipase. J. Biol. Chem. 1983 Aug 10;258(15):9197-9202.

42. Mattson FH, Volpenhein RA. Rate and extent of absorption of the fatty acids of fully esterified glycerol, erythritol, xylitol, and sucrose as measured in thoracic duct cannulated rats. J. Nutr. 1972 Sep;102(9):1177-1180.

43. Howles PN, Carter CP, Hui DY. Dietary Free and Esterified Cholesterol Absorption in Cholesterol Esterase (Bile Salt-stimulated Lipase) Gene-targeted Mice. Journal of Biological Chemistry. 1996 Mar 22;271(12):7196-7202.

44. Huggins KW, Camarota LM, Howles PN, Hui DY. Pancreatic Triglyceride Lipase Deficiency Minimally Affects Dietary Fat Absorption but Dramatically Decreases Dietary Cholesterol Absorption in Mice. Journal of Biological Chemistry. 2003 Oct 31;278(44):42899-42905.

45. Gilham D, Labonté ED, Rojas JC, Jandacek RJ, Howles PN, Hui DY. Carboxyl Ester Lipase Deficiency Exacerbates Dietary Lipid Absorption Abnormalities and Resistance to Diet-induced Obesity in Pancreatic Triglyceride Lipase Knockout Mice. Journal of Biological Chemistry. 2007;282(34):24642-24649.

46. P Tso, A Nauli, C-M Lo. Enterocyte fatty acid uptake and intestinal fatty acid-binding protein. Biochem. Soc. Trans. 2004 Feb;32(Pt 1):75-78.

47. Wilson FA, Sallee VL, Dietschy JM. Unstirred water layers in intestine: rate determinant of fatty acid absorption from micellar solutions. Science. 1971 Dec 3;174(13):1031-1033.

48. Kamp F, Hamilton JA, Kamp F, Westerhoff HV, Hamilton JA. Movement of fatty acids, fatty acid analogues, and bile acids across phospholipid bilayers. Biochemistry. 1993 Oct 19;32(41):11074-11086.

49. Chow SL, Hollander D. A dual, concentration-dependent absorption mechanism of linoleic acid by rat jejunum in vitro. J. Lipid Res. 1979 Mar;20(3):349-356.

50. Stremmel W, Lotz G, Strohmeyer G, Berk PD. Identification, isolation, and partial characterization of a fatty acid binding protein from rat jejunal microvillous membranes. J. Clin. Invest. 1985 Mar;75(3):1068-1076.

51. Stremmel W. Uptake of fatty acids by jejunal mucosal cells is mediated by a fatty acid binding membrane protein. J. Clin. Invest. 1988 Dec;82(6):2001-2010.

52. Schaffer JE, Lodish HF. Expression cloning and characterization of a novel adipocyte long chain fatty acid transport protein. Cell. 1994 Nov 4;79(3):427-436.

53. Stahl A, Hirsch DJ, Gimeno RE, Punreddy S, Ge P, Watson N, et al. Identification of the Major Intestinal Fatty Acid Transport Protein. Molecular Cell. 1999 Sep;4(3):299-308.

54. Ho S, Storch J. Common mechanisms of monoacylglycerol and fatty acid uptake by human intestinal Caco-2 cells. Am J Physiol Cell Physiol. 2001 Oct 1;281(4):C1106-1117.

55. Murota K, Storch J. Uptake of Micellar Long-Chain Fatty Acid and sn-2-Monoacylglycerol into Human Intestinal Caco-2 Cells Exhibits Characteristics of Protein-Mediated Transport. J. Nutr. 2005 Jul 1;135(7):1626-1630.

56. Stahl A. A current review of fatty acid transport proteins (SLC27). Pflugers Arch. 2004 Feb;447(5):722-727.

57. Abumrad NA, Sfeir Z, Connelly MA, Coburn C. Lipid transporters: membrane transport systems for cholesterol and fatty acids. Curr Opin Clin Nutr Metab Care. 2000 Jul;3(4):255-262.

58. Drover VA, Nguyen DV, Bastie CC, Darlington YF, Abumrad NA, Pessin JE, et al. CD36 mediates both cellular uptake of very long chain fatty acids and their intestinal absorption in mice. J. Biol. Chem. 2008 May 9;283(19):13108-13115.

59. Bass NM, Manning JA, Ockner RK, Gordon JI, Seetharam S, Alpers DH. Regulation of the biosynthesis of two distinct fatty acid-binding proteins in rat liver and intestine. Influences of sex difference and of clofibrate. Journal of Biological Chemistry. 1985 Feb 10;260(3):1432-1436.

60. Besnard P, Niot I, Bernard A, Carlier H. Cellular and Molecular Aspects of Fat Metabolism in the Small Intestine. Proceedings of the Nutrition Society. 1996;55(1B):19-37.

61. Bass NM. The cellular fatty acid binding proteins: aspects of structure, regulation, and function. Int. Rev. Cytol. 1988;111:143-184.

62. Cistola DP, Sacchettini JC, Banaszak LJ, Walsh MT, Gordon JI. Fatty acid interactions with rat intestinal and liver fatty acid-binding proteins expressed in Escherichia coli. A comparative 13C NMR study. Journal of Biological Chemistry. 1989 Feb 15;264(5):2700-2710.

63. Glatz JFC, van der Vusse GJ. Cellular fatty acid-binding proteins: Their function and physiological significance. Progress in Lipid Research. 1996 Sep;35(3):243-282.

64. Shields HM, Bates ML, Bass NM, Best CJ, Alpers DH, Ockner RK. Light microscopic immunocytochemical localization of hepatic and intestinal types of fatty acid-binding proteins in rat small intestine. J. Lipid Res. 1986 May;27(5):549-557.

65. Bell RM, Coleman RA. Enzymes of Glycerolipid Synthesis in Eukaryotes. Annu. Rev. Biochem. 1980 7;49(1):459-487.

66. Coleman RA, Lee DP. Enzymes of triacylglycerol synthesis and their regulation. Prog. Lipid Res. 2004 Mar;43(2):134-176.

67. Phan CT, Tso P. Intestinal lipid absorption and transport. Front. Biosci. 2001 Mar 1;6:D299-319.

68. Polheim D, David JSK, Schultz FM, Wylie MB, Johnston JM. Regulation of triglyceride biosynthesis in adipose and intestinal tissue. J. Lipid Res. 1973 Jul 1;14(4):415-421.

69. Johnston JM, Rao GA, Lowe PA. The separation of the alpha-glycerophosphate and monoglyceride pathways in the intestinal biosynthesis of triglycerides. Biochim. Biophys. Acta. 1967 Jun 6;137(3):578-580.

70. Kayden HJ, Senior JR, Mattson FH. The monoglyceride pathway of fat absorption in man. J. Clin. Invest. 1967 Nov;46(11):1695-1703.

71. Cases S, Smith SJ, Zheng Y, Myers HM, Lear SR, Sande E, et al. Identification of a gene encoding an acyl CoA:diacylglycerol acyltransferase, a key enzyme in triacylglycerol synthesis. Proceedings of the National Academy of Sciences of the United States of America. 1998 Oct 27;95(22):13018-13023.

72. Cao J, Hawkins E, Brozinick J, Liu X, Zhang H, Burn P, et al. A Predominant Role of Acyl-CoA:monoacylglycerol Acyltransferase-2 in Dietary Fat Absorption Implicated by Tissue Distribution, Subcellular Localization, and Up-regulation by High Fat Diet. Journal of Biological Chemistry. 2004 Apr 30;279(18):18878-18886.

73. Cao J, Cheng L, Shi Y. Catalytic properties of MGAT3, a putative triacylgycerol synthase. J. Lipid Res. 2007 Mar 1;48(3):583-591.

74. Yen CE, Stone SJ, Cases S, Zhou P, Farese RV. Identification of a gene encoding MGAT1, a monoacylglycerol acyltransferase. Proc. Natl. Acad. Sci. U.S.A. 2002 Jun 25;99(13):8512-8517.

75. Cao J, Lockwood J, Burn P, Shi Y. Cloning and Functional Characterization of a Mouse Intestinal Acyl-CoA:Monoacylglycerol Acyltransferase, MGAT2. Journal of Biological Chemistry. 2003 Apr 18;278(16):13860-13866.

76. Cheng D, Nelson TC, Chen J, Walker SG, Wardwell-Swanson J, Meegalla R, et al. Identification of Acyl Coenzyme A:Monoacylglycerol Acyltransferase 3, an Intestinal Specific Enzyme Implicated in Dietary Fat Absorption. Journal of Biological Chemistry. 2003 Apr 18;278(16):13611-13614.

77. Yen CE, Farese RV. MGAT2, a Monoacylglycerol Acyltransferase Expressed in the Small Intestine. Journal of Biological Chemistry. 2003 May 16;278(20):18532-18537.

78. Yen CE, Stone SJ, Cases S, Zhou P, Farese RV. Identification of a gene encoding MGAT1, a monoacylglycerol acyltransferase. Proc Natl Acad Sci U S A. 2002 Jun 25;99(13):8512-8517.

79. Yen CE, Cheong M, Grueter C, Zhou P, Moriwaki J, Wong JS, et al. Deficiency of the intestinal enzyme acyl CoA:monoacylglycerol acyltransferase-2 protects mice from metabolic disorders induced by high-fat feeding. Nat Med. 2009 Apr;15(4):442-446.

80. Lockwood JF, Cao J, Burn P, Shi Y. Human intestinal monoacylglycerol acyltransferase: differential features in tissue expression and activity. Am J Physiol Endocrinol Metab. 2003 Nov 1;285(5):E927-937.

81. Cases S, Stone SJ, Zhou P, Yen E, Tow B, Lardizabal KD, et al. Cloning of DGAT2, a Second Mammalian Diacylglycerol Acyltransferase, and Related Family Members. Journal of Biological Chemistry. 2001 Oct 19;276(42):38870-38876.

82. Owen MR, Corstorphine CC, Zammit VA. Overt and latent activities of diacylglycerol acytransferase in rat liver microsomes: possible roles in very-low-density lipoprotein triacylglycerol secretion. Biochem. J. 1997 Apr 1;323 (Pt 1):17-21.

83. Waterman IJ, Zammit VA. Activities of overt and latent diacylglycerol acyltransferases (DGATs I and II) in liver microsomes of ob/ob mice. Int. J. Obes. Relat. Metab. Disord. 2002 May;26(5):742-743.

84. Cheng D, Iqbal J, Devenny J, Chu C, Chen L, Dong J, et al. Acylation of Acylglycerols by Acyl Coenzyme A:Diacylglycerol Acyltransferase 1 (DGAT1). Journal of Biological Chemistry. 2008 Oct 31;283(44):29802-29811.

85. Yen CE, Monetti M, Burri BJ, Farese RV. The triacylglycerol synthesis enzyme DGAT1 also catalyzes the synthesis of diacylglycerols, waxes, and retinyl esters. J. Lipid Res. 2005 Jul 1;46(7):1502-1511.

86. Buhman KK, Smith SJ, Stone SJ, Repa JJ, Wong JS, Knapp FF, et al. DGAT1 is not essential for intestinal triacylglycerol absorption or chylomicron synthesis. J. Biol. Chem. 2002 Jul 12;277(28):25474-25479.

87. Smith SJ, Cases S, Jensen DR, Chen HC, Sande E, Tow B, et al. Obesity resistance and multiple mechanisms of triglyceride synthesis in mice lacking Dgat. Nat. Genet. 2000 May;25(1):87-90.

88. Lehner R, Kuksis A. Triacylglycerol synthesis by an sn-1,2(2,3)-diacylglycerol transacylase from rat intestinal microsomes. J. Biol. Chem. 1993 Apr 25;268(12):8781-8786.

89. Stone SJ, Myers HM, Watkins SM, Brown BE, Feingold KR, Elias PM, et al. Lipopenia and Skin Barrier Abnormalities in DGAT2-deficient Mice. Journal of Biological Chemistry. 2004 Mar 19;279(12):11767-11776.

90. De Jong BJ, Kalkman C, Hülsmann WC. Partial purification and properties of monoacylglycerol lipase and two esterases from isolated rat small intestinal epithelial cells. Biochim. Biophys. Acta. 1978 Jul 25;530(1):56-66.

91. Pope JL, McPherson JC, Tidwell HC. A study of a monoglyceride-hydrolyzing enzyme of intestinal mucosa. J. Biol. Chem. 1966 May 25;241(10):2306-2310.

92. Tornqvist H, Belfrage P. Purification and some properties of a monoacylglycerol-hydrolyzing enzyme of rat adipose tissue. J. Biol. Chem. 1976 Feb 10;251(3):813-819.

93. Fredrikson G, Tornqvist H, Belfrage P. Hormone-sensitive lipase and monoacylglycerol lipase are both required for complete degradation of adipocyte triacylglycerol. Biochim. Biophys. Acta. 1986 Apr 15;876(2):288-293.

94. Tornqvist H, Nilsson-Ehle P, Belfrage P. Enzymes catalyzing the hydrolysis of long-chain monoacyglycerols in rat adipose tissue. Biochim. Biophys. Acta. 1978 Sep 28;530(3):474-486.

95. Karlsson M, Contreras JA, Hellman U, Tornqvist H, Holm C. cDNA Cloning, Tissue Distribution, and Identification of the Catalytic Triad of Monoglyceride Lipase. Journal of Biological Chemistry. 1997 Oct 24;272(43):27218-27223.

96. Ho S, Delgado L, Storch J. Monoacylglycerol metabolism in human intestinal Caco-2 cells: evidence for metabolic compartmentation and hydrolysis. J. Biol. Chem. 2002 Jan 18;277(3):1816-1823.

97. Chon S, Zhou YX, Dixon JL, Storch J. Intestinal monoacylglycerol metabolism: developmental and nutritional regulation of monoacylglycerol lipase and monoacylglycerol acyltransferase. J. Biol. Chem. 2007 Nov 16;282(46):33346-33357.

98. Coleman R, Haynes E. Hepatic monoacylglycerol acyltransferase. Characterization of an

activity associated with the suckling period in rats. J. Biol. Chem. 1984 Jul 25;259:8934-8938.

99. Bradford M. A rapid and sensitive method for the quantitation ... [Anal Biochem. 1976] - PubMed result. Anal. Biochem. 1976;72:248-254.

100. Chon S, Zhou YX, Dixon JL, Storch J. Intestinal Monoacylglycerol Metabolism: DEVELOPMENTAL AND NUTRITIONAL REGULATION OF MONOACYLGLYCEROL LIPASE AND MONOACYLGLYCEROL ACYLTRANSFERASE. J. Biol. Chem. 2007 Nov 16;282(46):33346-33357.

101. Trotter PJ, Ho SY, Storch J. Fatty acid uptake by Caco-2 human intestinal cells. J. Lipid Res. 1996 Feb;37(2):336-346.

102. Bligh E, Dyer W. A rapid method of total lipid extraction and purification. Can J Biochem Physiol. 1959 Aug;37:911-917.

103. Yen CE, Stone SJ, Cases S, Farese RV. Identification of a gene encoding MGAT1, a monoacylglycerol acyltransferase. PNAS. 2002 Jun 25;99:8512-8517.

104. Trotter PJ, Storch J. Fatty acid esterification during differentiation of the human intestinal cell line Caco-2. J. Biol. Chem. 1993 May 15;268(14):10017-10023.

105. Hülsmann WC, Kurpershoek-Davidov R. Topographic distribution of enzymes involved in glycerolipid synthesis in rat small, intestinal epithelium. Biochim. Biophys. Acta. 1976 Dec 20;450(3):288-300.

106. Chon S, Zhou YX, Quadro L, Storch J. Over-expression of monoacylglycerol lipase (MGL) in mouse small intestine results in an obese phenotype. The FASEB Journal: Official Publication of the Federation of American Societies for Experimental Biology. 2008 Mar 1;22:807.12.

107. Storch J, McDermott L. Fatty acid binding proteins and fatty acid transprot. In: Duttaroy AK, Spener F, editors. Cellular proteins and their fatty acids in health and disease. Wiley-VCH; 2003. p. 119-133.

108. Xia T, Mostafa N, Bhat BG, Florant GL, Coleman RA. Selective retention of essential fatty acids: the role of hepatic monoacylglycerol acyltransferase. Am. J. Physiol. 1993 Aug;265(2 Pt 2):R414-419.

109. Johnston JM, Rao GA, Lowe PA, Schwarz BE. The nature of the stimulatory role of the supernatant fraction on triglyceride synthesis by the alpha-Glycerophosphate pathway. Lipids. 1967 Jan;2(1):14-20.

110. Pelech SL, Vance DE. Regulation of phosphatidylcholine biosynthesis. Biochimica et Biophysica Acta (BBA) - Reviews on Biomembranes. 1984 Jun 25;779(2):217-251.